DOCTORAL THESIS

SHIBAURA INSTITUTE OF TECHNOLOGY

INVESTIGATION OF CATHETER'S CONTACT FORCE AND ANGLE EFFECTS ON CONTACT AREA AND LESION SIZE IN RADIOFREQUENCY CATHETER CARDIAC ABLATION

2021/September

Kriengsak Masnok

INVESTIGATION OF CATHETER'S CONTACT FORCE AND ANGLE EFFECTS ON CONTACT AREA AND LESION SIZE IN RADIOFREQUENCY CATHETER CARDIAC ABLATION

Kriengsak Masnok

Functional Control systems
Graduate School of Engineering and Sciences

Submitted in partial fulfilment of the requirements for the degree of

Doctor of Engineering

Shibaura Institute of Technology

2021/September

Acknowledgements

Foremost, I would like to start by expressing my sincere gratitude to my magnificent supervisor, Assoc. Prof. Dr. Nobuo Watanabe. The work present in this thesis would not have been possible without his expertise, patience, support, and, importantly, the great effort he put into establishing an academic infrastructure designed to allow me to grow up. I am also thankful to the Ministry of Education, Culture, Sports, Science and Technology (MEXT) Japan and Shibaura Institute of Technology for supporting the scholarships and research expenses. I also would like to thank all the Biofluid Science & Engineering Laboratory members who are always helping me. I would like to thank Boston Scientific Japan for their kind provision of catheters and RF devices. I would also like to express my gratitude to Mr. Kiyofumi Takahashi and Mr. Hiroyuki Arita from Boston Scientific Japan for their advice and support.

Finally, to my parent, words cannot express how grateful I am for your love, support, and encouragement. Thank you for giving me the strength to follow my dream and for supporting me.

Abstract

Over the past three decades, radiofrequency (RF) catheter ablation therapy has become a widely used and effective treatment for some cardiac arrhythmias. Catheter contact force and contact angle are well known as the factors that influence the size of the lesion produced during ablation. However, it was unknown exactly in detail how these factors influence each ablation dimension. Moreover, the relationships between various parameters and lesion dimensions are still indefinite, especially the relationship between contact area and lesion area as the function of catheter contact force and angle. Accordingly, this research aimed to investigate the effects of catheter contact force and contact angle on contact area and lesion size in radiofrequency catheter cardiac ablation. The work presented in this thesis was divided into two main parts;

The first part focused on investigates the effects of catheter contact force and contact angle on the catheter contact area. The main objectives of this part were to develop an experimental procedure for setting the catheter angle with respect to the surface of the heart muscle and the catheter contact force, as well as to investigate the catheter contact area on the heart muscle as a function of catheter contact angle and contact force. This present study successfully developed the experimental system that enables us to set the precision catheter contact angle with respect to the heart muscle's surface and the catheter contact force. This study showed that the present experimental system has feasibility for use to study radiofrequency catheter ablation. The findings can be summarized as follows; First, the morphology of the contact area can be divided into four types: rectangular, circular, ellipsoidal, and semi-ellipsoidal. Second, the morphology of the contact area indicates that the correlation between contact force and the contact area is a logarithmic function; that is, increased contact force was associated with increased contact area, and the contact angle has as strong an effect on the contact area as contact force does. Last, there is an inverse correlation between

contact angle and contact area; a smaller contact angle is associated with increased contact area.

The second part of this thesis deals with the challenges to investigating the effects of catheter contact force and contact angle on the ablation lesion dimensions and investigating the effect of catheter contact force and contact angle on the ablation lesion dimension and the ablation impedance. In addition, this part also aims to investigate the relationship between the catheter contact area and the dimensions of the ablation lesion as a function of catheter contact angle and force in the radiofrequency catheter ablation process. This study showed an important role of the catheter contact force on the ablation lesion and impedance in RF catheter ablation procedures. The results showed that the catheter contact force has a significant correlation with ablation impedance, but the ablation impedance did not significantly differ with each catheter contact angle. In addition, the results revealed that the catheter contact area showed a strong correlation with the ablation lesion area. When the contact area was increased, the lesion area also increased linearly in a monotonic manner. The relationships between catheter contact force and ablation lesion area and between catheter contact force and ablation lesion depth are logarithmic functions in which increased contact force was associated with increased lesion area and depth. Lastly, the catheter contact angle is also an important determinant of the lesion area. The lesion area progressively increased when the contact angle was decreased. In contrast, the lesion depth progressively increased when the contact angle was increased.

Such information should be helpful in the selection of effective values for contact force and contact angle in order to predict lesion size as well as for clinicians performing this procedure to understand the relationships among the parameters and plan their ablation strategy accordingly.

Table of Contents

List of Figures

List of Tables

List of Abbreviations & Symbols

RF	Radiofrequency
SCD	Sudden cardiac death
ECG	Electrocardiogram
AAD	Anti-arrhythmia drug
EP	Electrophysiology
AC	Alternating circuit
DC	Direct circuit
P	Power
I	Current
R	Resistant
Imp	Impedance
W	Watt
Ω	Ohm
SA Node	Sinoatrial Node
A-V Node	Atrioventricular Node
VT	Ventricular tachycardia
SVT	Supraventricular tachycardia
SSS	Sick sinus syndrome
AT	Atrial tachycardia
AF	Atrial fibrillation
VF	Ventricular fibrillation
N	Newton
g	gram
gf	Gram-force
Hz	Hertz
kHz	Kilohertz
wt%	Percentage by weight
mm	Millimetre
cm	Centimetre
mL	Millilitre
Fr	French scale

deg	Degree
h	Hour
min	Minute
sec	Second
s	Second
T	Type
C	Concentration
℃	Celsius
AVG	Average
Max	Maximum
Min	Minimum
SD	Standard deviation
CV	Coefficient of variation
AVG CA	Average contact area
PCA	Percentage contact area
R^2	Coefficient of determination
r	Pearson's coefficient
r_s	Spearman's coefficient
Log	Logarithmic

Chapter 1: Introduction

This chapter outlines the research background (section 1.1) and its objectives (section 1.2). Section 1.3 describes the scope of this research and provides definitions of the terms used. Finally, section 1.4 includes an outline of the remaining chapters of the thesis.

1.1 BACKGROUND

Cardiac arrhythmias affect millions of people. The World Health Organization (WHO) reported nearly 17.9 million global deaths due to cardiovascular disease every year [1]. It is estimated that about 40-50% of all cardiovascular disease deaths are sudden cardiac death (SCDs), and about 80% of SDCs result from ventricular tachyarrhythmias. Therefore, about 6 million sudden cardiac deaths occur annually due to ventricular tachyarrhythmias. Moreover, some studies reported that approximately 6% of the population over the age of 65 has atrial fibrillation, and the number approaches 10% in people over the age of 85. Estimates of the prevalence of only atrial fibrillation in the United States extend from about 2.7 million to 6.1 million. That number is estimated to double to 12.1 million in 2030. Global, the expected number of individuals with atrial fibrillation in 2010 was 33.5 million, according to a 2013 study [2]. That is about 0.5 percent of the world's population. These data showed only a few cardiac arrhythmias even exclude other types, but it has revealed the widespread impact on the public health care system and many people worldwide.

The treatment techniques for cardiac arrhythmias are constantly being developed. Over the past three decades, radiofrequency (RF) catheter ablation therapy has become a widely used and effective treatment for some cardiac arrhythmias. However, there is still important information that requires further elucidation in many details to fulfill the knowledge in this research field. This present study focuses on investigating the effects of catheter contact force and contact angle on contact area and

lesion size in radiofrequency catheter cardiac ablation. These data should be helpful in the selection of effective values for contact force and contact angle with the aim of reducing risk in the clinical application of RF ablation and should also be useful for those performing this procedure to understand the relationships among the parameters and plan their treatment strategy beforehand.

1.2 RESEARCH OBJECTIVES

This research embarks on the following objectives:

- Develop an experimental procedure for setting the catheter angle with respect to the surface of the heart muscle and the catheter contact force, as well as to investigate the catheter contact area on the heart muscle as a function of catheter contact angle and contact force.
- Investigate the effect of catheter contact force and contact angle on the ablation lesion dimension and the ablation impedance.
- Investigate the relationship between the catheter contact area and the dimensions of the ablation lesion as a function of catheter contact angle and force in the radiofrequency catheter ablation process.

1.3 SCOPE AND DEFINITIONS

- The term "in vitro" and "ex vivo" are frequently used in the field of catheter ablation research, as both testing methods involve experiments on biological matter conducted outside of a living organism and in an artificial environment. Therefore, this study used both terms.
- The standard SI unit for force is the newton (N), but gram-force (gf) is frequently used to measure contact force in the field of catheter ablation research (1 gf = 0.00981 N, which is the force acting on a mass of 1 g under the Earth's gravitational acceleration of 9.81 m/s^2). Therefore, this study used gf as a unit for force.

1.4 THESIS OUTLINE

The title of this research is “Investigation of Catheter’s Contact Force and Angle Effects on Contact Area and Lesion Size in Radiofrequency Catheter Cardiac Ablation” This section briefly describes the content of the research thesis which consist of five deferent chapter including Introduction, Literature Review, Effects of Catheter Contact Force and Angle on Contact Area, Effects of Catheter Contact Force and Angle on Lesion Area, and Conclusions and Future Work

- **Chapter 1:** The first chapter provides the research background (section 1.1) and its objectives (section 1.2). Section 1.3 describes the scope of this research and provides definitions of the terms used. Finally, section 1.4 includes an outline of the remaining chapters of the thesis.
- **Chapter 2:** The second chapter provides the literature review of this research begins with an overview of basic mechanisms of cardiac arrhythmias (section 2.1), including the electrical system of the heart (section 2.1.1) and principal mechanisms of cardiac arrhythmias (section 2.1.2). Then, briefly describe the radiofrequency catheter ablation of cardiac arrhythmias (section 2.2), including; the overview of the RF catheter cardiac ablation procedure (section 2.2.1), physical aspects (section 2.2.2), mechanism of lesion formation by RF current (section 2.2.3), and types of RF catheter ablation (section 2.2.4). Section 2.3 highlights the role of the contact force and contact angle in catheter ablation of cardiac arrhythmias, including; the factor that influences lesion dimensions (section 2.3.1) and the importance of catheter contact force and contact angle (section 2.3.2.). Lastly is the summary of the literature review of this research (section 2.4)
- **Chapter 3:** The third chapter focused on investigates the effects of catheter contact force and contact angle on the catheter contact area. The topic is this chapter are including; Section 3.1 purpose of the study,

Section 3.2 methods, Section 3.3 results, Section 3.4 discussion, Section 3.5 major findings, Section 3.6 clinical implications, Section 3.7 study limitations, and Section 3.8 Conclusion.

- **Chapter 4:** The fourth chapter focused on investigates the effects of catheter contact force and angle on the ablation lesion dimension, ablation impedance, and their relationship. The topic is this chapter are including; Section 4.1 purpose of the study, Section 4.2 methods, Section 4.3 results, Section 4.4 discussion, Section 4.5 major findings, Section 4.6 clinical implications, Section 4.7 study limitations, and Section 4.8 Conclusion.
- **Chapter 5:** The fifth chapter deliver the future work of this study including further application and further research.
- **Chapter 6:** The last chapter deliver the conclusion of the entire research.

Chapter 2: Literature Review

This chapter begins with an overview of basic mechanisms of cardiac arrhythmias (section 2.1), including the electrical system of the heart (section 2.1.1) and principal mechanisms of cardiac arrhythmias (section 2.1.2). Then, briefly describe the radiofrequency catheter ablation of cardiac arrhythmias (section 2.2), including; the overview of the RF catheter cardiac ablation procedure (section 2.2.1), physical aspects (section 2.2.2), mechanism of lesion formation by RF current (section 2.2.3), and types of RF catheter ablation (section 2.2.4). Section 2.3 highlights the role of the contact force and contact angle in catheter ablation of cardiac arrhythmias, including; the factor that influences lesion dimensions (section 2.3.1) and the importance of catheter contact force and contact angle (section 2.3.2.). Lastly is the summary of the literature review of this research (section 2.4)

2.1 OVERVIEW OF BASIC MECHANISMS OF CARDIAC ARRHYTHMIAS

2.1.1 Electrical system of the heart

The heartbeat is initiate by an intrinsic electrical system composed of modified myocytes, not nerves. As shown in Figure 1., the electrical signal travels through the network of conducting cell "pathways" generated from the sinoatrial node (SA Node). SA node is the natural pacemaker located in the upper portion of the right atrium. Next, the electrical impulse travels to the atrioventricular node or "A-V node," located between the atria from the sinus node. There, impulses are slowed down for a concise period then the electrical impulse travels through the bundle of His. The bundle of His divides into right and left, called bundle branches, stimulates the right and left ventricles. The electrical impulse enters the ventricles' muscles, then contracts and produces a heartbeat [3]. Measuring electrical heart information is often used Electrocardiography (ECG) alongside other tests. An ECG is a graph of voltage with respect to time that reflects the electrical activities of cardiac muscle depolarization

followed by repolarization during each heartbeat. The ECG graph of a regular beat (shown in Figure 2.) consists of a sequence of waves, a P-wave presenting the atrial depolarization process, a QRS complex denoting the ventricular depolarization process, and a T-wave representing the ventricular repolarization. Other portions of the signal include the PR, ST, and QT intervals. The ECG is also invaluable for diagnosing cardiac arrhythmias, especially before an intracardiac electrophysiology (EP) [3, 4].

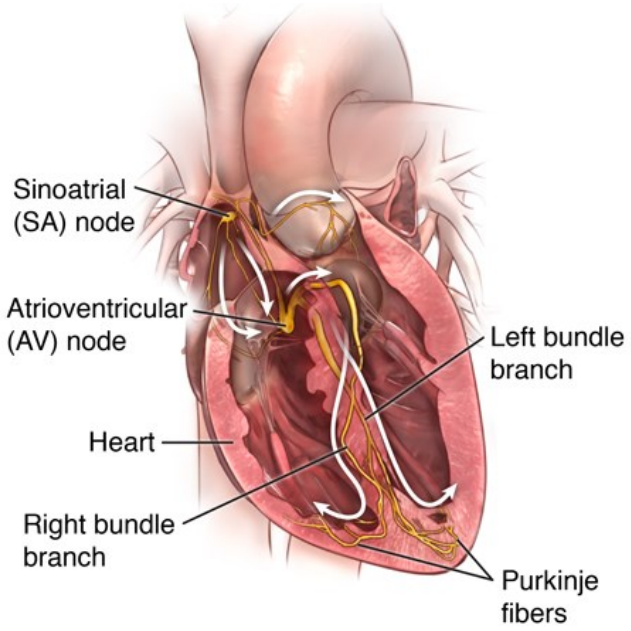

Figure 1. Illustration of a human heart showing basic structure and electrical system of the heart. Taken from: https://www.hopkinsmedicine.org/health/conditions-and-diseases/anatomy-and-function-of-the-hearts-electrical-system

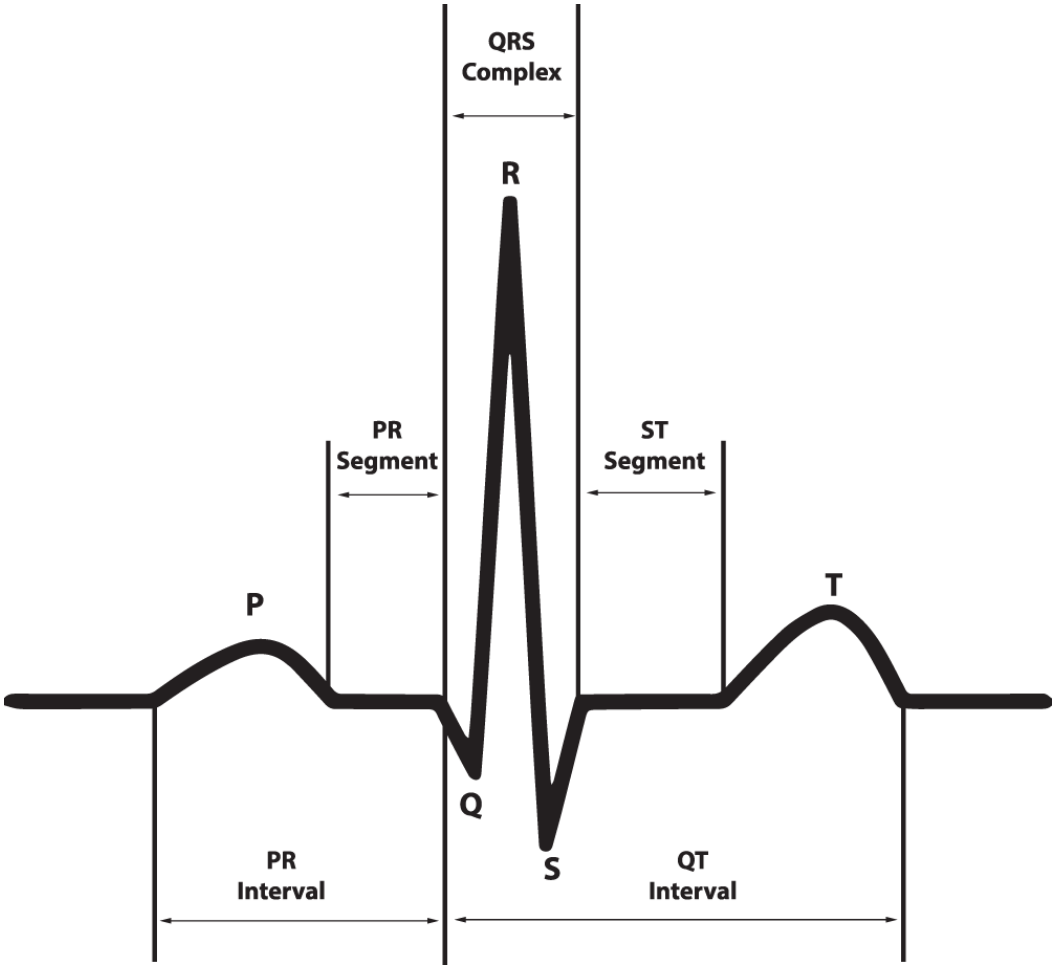

Figure 2. The ECG waveform of a normal heart beat [4].

2.1.2 Principal Mechanisms of Cardiac Arrhythmias

A cardiac arrhythmia is defined as a variation from the regular heart rate and/or rhythm that is not physiologically justified. Cardiac arrhythmias are caused by the mechanism alterations responsible divided into disorders of impulse formation, disorders of impulse conduction, or a combination of both through the myocardial tissue, which may modify the origin and physiological diffusion of the electrical stimulus of the heart. They indicate a disturbance of the heart rhythm, varying in severity from entirely benign to arrhythmias with an immediate risk of life [5, 6]. There are many ways to classify cardiac arrhythmias, such as classified according to their electrophysiological mechanism, their point of origin in the myocardial tissue, the appearance of a causal condition or its apparent absence, the appearance or absence of impaired myocardial function, the specific clinical features of tachycardia or

bradycardia, the electrocardiographic pattern, the relationships with the autonomic nervous system and the sensitivity to the various categories of drugs [7]. However, it is common for all to be classified in two principal ways. The first is classified according to the originates sources, such as ventricular tachycardia (VT) originating in the lower chambers of the heart (ventricles) or supraventricular tachycardia (SVT) originating above the ventricles (supraventricular) in the atria or AV node. The second is classified according to resulting heart rate with bradycardia indicating heartbeats lower than 60 times a minute, such as sick sinus syndrome (SSS) and atrioventricular (AV) conduction block. Tachycardia indicating a heart rate of more than 100 times a minute, such as atrial tachycardia (AT), atrial fibrillation (AF), and ventricular fibrillation (VF) [5, 8]. Almost 80% of SDCs occur in patients with ischemic heart disease or heart failure. These patients present genetically-based or inherited cardiac arrhythmias [2]. The most common arrhythmia was AV block, which was followed by ventricular tachycardia and atrial fibrillation, while the most common cause of SCD is ventricular tachycardia that degenerates into ventricular fibrillation [9–11].

2.2 RADIOFREQUENCY CATHETER ABLATION OF CARDIAC ARRHYTHMIAS

Drug therapy is generally used as the first-line for the treatment of cardiac arrhythmias patients. However, one major limitation of drug therapy to control rhythm in arrhythmias patients is the ineffectiveness, and long-term use of these drugs may cause adverse side effects associated with anti-arrhythmias drugs (AADs) [12, 13]. The era of radiofrequency (RF) ablative therapy of cardiac arrhythmias began in 1987 when Borggrefe M et al. and Huang Sk et al. performed for the first time in the treatment of an arrhythmia incorporating an accessory pathway in a human [14, 15]. Soon after the introduction of the RF ablation technique, RF catheter ablation has rapidly emerged as the effective minimally invasive treatment of choice for some cardiac arrhythmias. Due to eliminates the requirement for open-heart surgery or long-term medication and safe [16–20].

2.2.1 Overview of the RF catheter cardiac ablation procedure

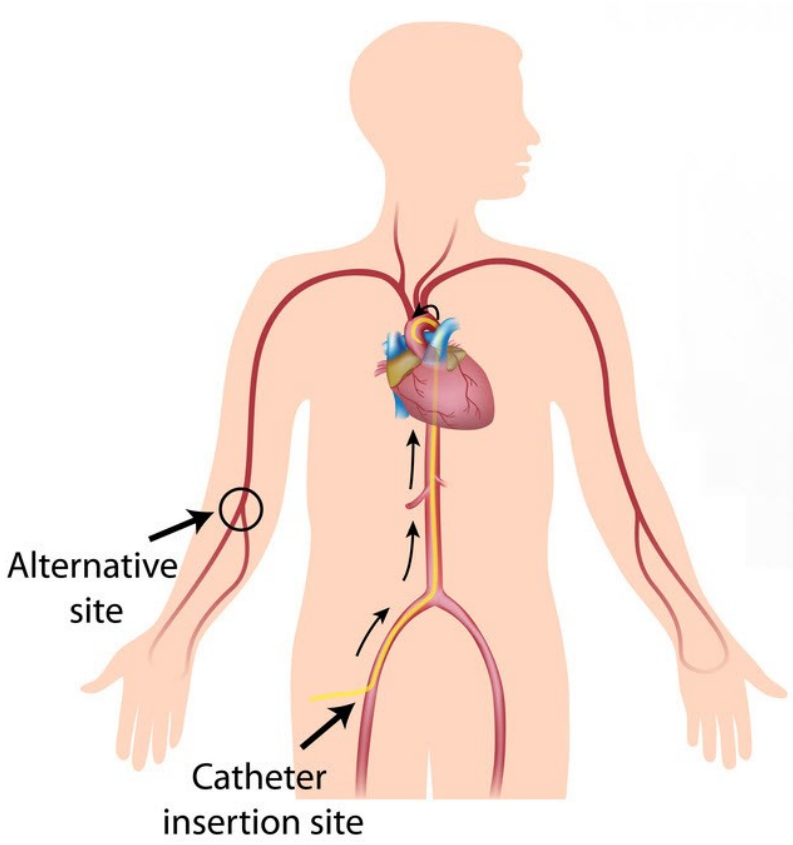

Figure 3. Catheter insertion points for cardiac ablation. Taken from: https://www.columbiaindiahospitals.com/health-articles/cardiac-ablation-procedure

In general, all ablative-type therapies for cardiac arrhythmias consist of the delivery of some source of energy within the heart at such a magnitude that it causes local myocardial destruction of anatomic regions critical for abnormal impulse generation and/or propagation. The ultimate aim of these destructive lesions is either silencing the foci responsible for abnormal automaticity or interruption of the re-entry circuits responsible for arrhythmia genesis or continuation. During the standard RF catheter cardiac ablation procedure, the catheters were inserted into the heart via a blood vessel through the groin or alternative site, as shown in Figure 3. Using various modalities and catheter navigation technology such as fluoroscopy and electromagnetic guidance, an electrophysiologist (EP) manipulates the catheter to a specific heart's target area. After the catheter tip is positioned at the heart's target area,

the sensor on the catheter's tip electrode sends electrical impulses and record heart electricity. This information was used to identify the area that is causing the arrhythmia. Then, the RF energy was applied to create a small lesion on the heart and block or adjust the electrical pathways [21].

2.2.2 Physical Aspects

The RF current frequency, mostly used in the ablation of cardiac arrhythmias, is 300 to 1000 kHz. Lower frequency alternating current (<100kHz) usually stimulates excitable cells and produces pain and muscle contractions or ventricular fibrillation when applied to the myocardium. During the RF catheter ablation process, the RF generator generated the energy is then delivered from the tip electrode of an ablation catheter passes through the contact area on the heart tissue surface and blood. The high density of alternating current that passes through the resistive tissue generates heat and raises the tissue temperature. Figure 4. shown illustrates the ablation biophysics process from the initial phase until the lesion occurred. At the initial phase, resistive heating starts simultaneously as the electrical current flows into the heart tissue surface. The temperature is then transferred to the surrounding tissue by conduction and radiation [22, 23]. Once this temperature exceeds ≈50-55°C, the cells in that contact area undergo necrosis [24–28]. The ablation resistance can be considered into two components. The first is the resistance between the catheter tip and the heart tissue surface. The second is the resistance between the catheter tip and blood. The relationship between power, current, and resistance (or impedance in terms of AC circuit) in the RF catheter ablation process can be expressed by Ohm's law, whereas power (P) equals current squared (I^2) multiplied by resistance (R): $P=I^2R$, as shown in Figure 5.

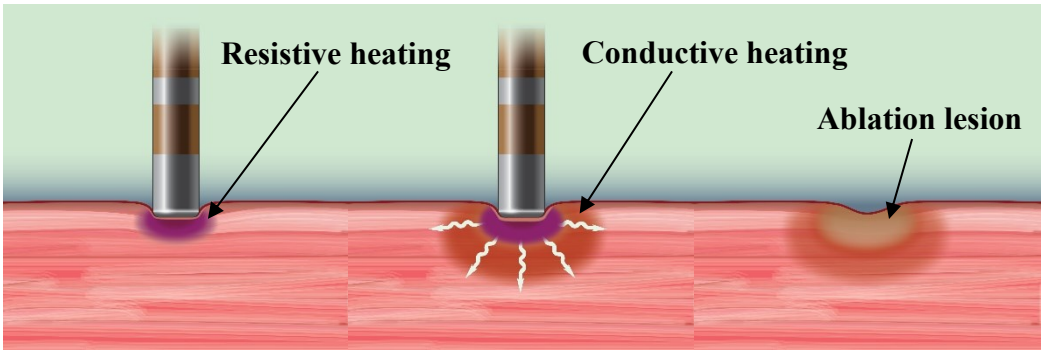

Figure 4. The ablation biophysics process from the initial phase until the lesion occurred.

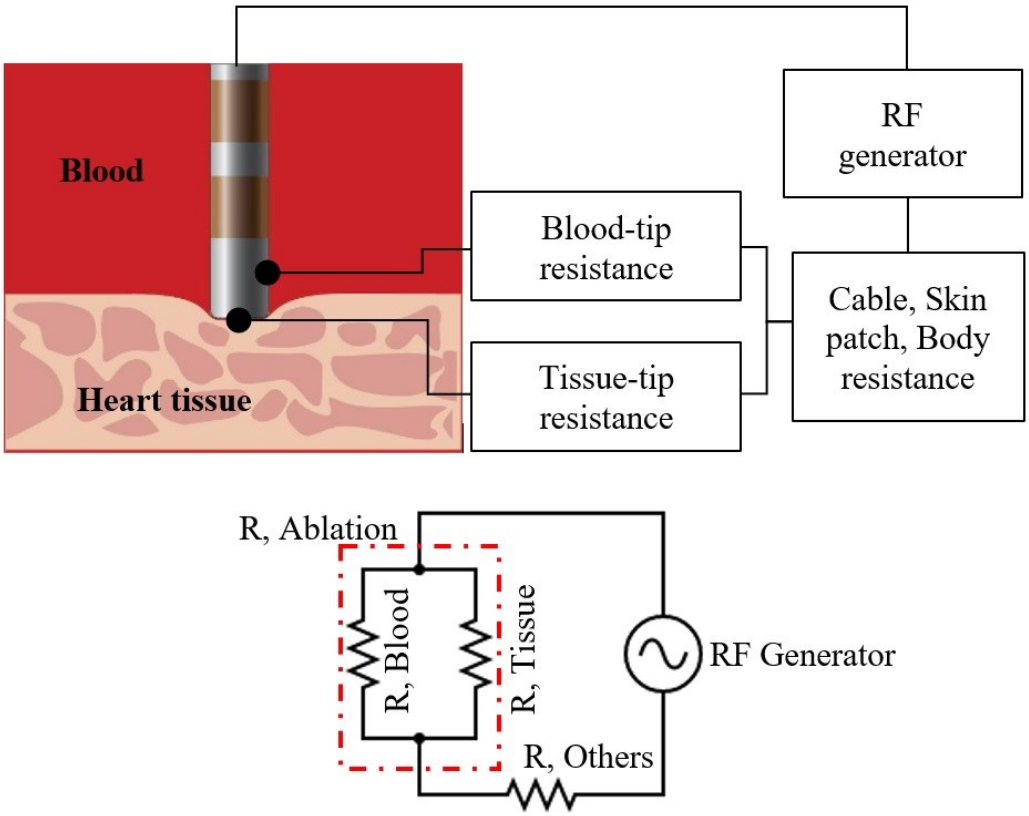

Figure 5. Schematic representation of the electrical circuit path during RF ablation process.

2.2.3 Mechanism of lesion formation by RF current

It is well known that the goal of RF catheter ablation therapy is to create ablation lesions on the surface of the cardiac tissue to interrupt or adjust the transmission of the electrical signals. The effect of RF current can consider the ablation lesion formation. The effect of RF current on myocardial tissue is mediated by two factors: current itself (direct current shocks) and the thermal effect. The direct current shocks cause cellular depolarization and loss of automaticity [29, 30]. When heart tissue was shocks with current, micropores in the sarcolemma membrane potentially reflecting dielectric breakdown. Micropores are transient and are closed by self-reparatory properties of the plasma membrane so that viability is restored [31]. As a result of the thermal effect of RF current application, hyperthermia has a multitude of metabolic, electrophysiological, and structural effects on the cell. Metabolic effects of hyperthermia are mediated primarily by the sensitivity of various enzymes to temperature. Nath et al. and M. Dewhirst et al. have shown that hyperthermia causes a reversible loss of excitability in the temperature range 42.7 to 51.8℃ and irreversible loss of excitability for temperatures greater than 50℃ [22, 23, 27]. Therefore, in order to produce irreversible cellular change or death, the tissue must be heated up to at least 50℃, and sarcolemmal disruption seems to be a major mechanism through which cell death occurs and lesion formation during RF ablation.

2.2.4 Types of RF catheter ablation

In recent years, various RF catheters have been developed to increase ablation efficiency while minimizing risks for complications. RF catheter types are typically defined by the size of the catheter tip and the irrigation technology. At present, RF ablation catheters can be classified into four major types as suggested by Müssigbrodt et al., [32];

(1) standard 4 mm tip catheters,

(2) large 8-10 mm tip catheters,

(3) open-loop irrigated tip catheters,

(4) closed-loop irrigated tip catheters.

In clinical practice, open-loop irrigated and closed-loop catheter tips are mostly used. These different technologies include increased electrode size for enchanted passive cooling via the blood flow and active cooling of electrode through saline fluid cooling either internally (closed-loop) or eternally (open-loop), as shown in Figure 6. The non-irrigated catheters (4 and 8-10 mm) have several disadvantages and limitations such as reduce impedance feedback with possible excessive tissue heating, blood coagulum formation, impedance rise at a relatively low power level, and high temperature at the electrode-tissue interface (contact area). In comparison, the clinical efficiency of open-loop irrigated catheters is well established in clinical practice as it decreases the risk for thrombus formation, char formation, and cardiac perforating (steam pop) [33–36]

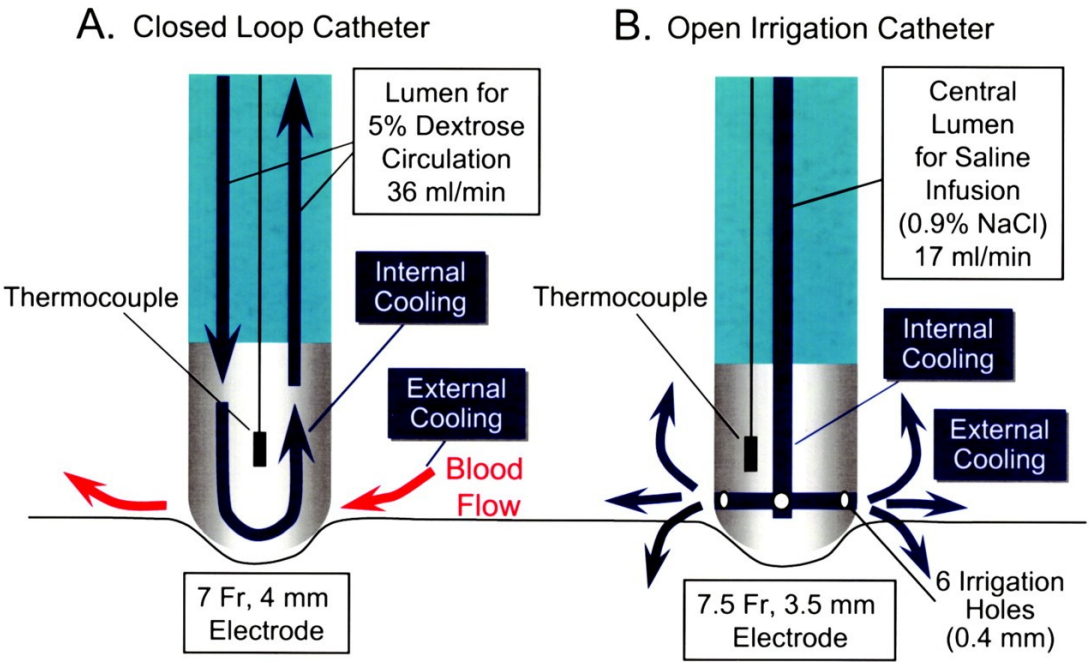

Figure 6. Schematic representation of the irrigated electrode catheters. **(a)**, Closed loop irrigation catheter has 7Fr, 4-mm tip electrode **(b)**, Open irrigation catheter has 7.5Fr, 3.5-mm tip electrode [35].

2.3 ROLE OF THE CONTACT FORCE AND CONTACT ANGLE IN CATHETER ABLATION OF CARDIAC ARRHYTHMIAS

2.3.1 Factors that influence lesion dimension

The study of factors that affect the size of the lesion is of great importance in the treatment of arrhythmia with catheter RF ablation. A deep understanding of these factors' mechanisms allows doctors to predict lesion size before starting the operation process, reducing the risk and increase treatment effectiveness. Several studies have revealed several factors that influence lesion dimensions, evaluated in terms of ablated area, volume, and depth [34, 37–39]. These factors are divided into two groups: active factor (controllable factor) and passive factor (uncontrollable factor). Active factors include as follows; electrical power [40–42], energy delivery [43, 44], catheter diameter [32, 45], exposure time [40, 46], ablation electrode temperature [47, 48], irrigation saline flow amount [33, 34, 42, 49] and contact force [39–41, 49–51]. Passive factors include as follows; ablation circuit impedance [39, 46], blood flow near the myocardial surface [44, 52–54], tissue thickness [44], and tissue architecture [55]. Among these factors, the catheter contact force is reported to show a strong positive correlation with lesion size [49–51, 56–58].

2.3.2 Important of catheter contact force and angle

Catheter contact force has been used as one of the most reliable parameters to predict lesion formation. Recently, catheter contact force was applied to combined with serval index for predict lesion dimensions such as force-time integral (FTI) calculated from the ablation time and contact force [59, 60], ablation index (AI) calculated from ablation time, ablation power, and contact force [59, 61] and lesion size index (LSI) calculated from ablation power, ablation time, and contact force with lesion dimension [62].

However, catheter contact force must be considered related to contact angle. During radiofrequency cardiac catheter ablation, the catheter electrode tip should contact the heart tissue surface at various angles. Thus, force must be defined with reference to the degree of tissue contact (or contact angle). Catheter contact force and

catheter orientation relative to heart tissue play an important role in determining lesion dimension, and they are directly linked to ablation efficacy and safety. The catheter tip electrode must contact the heart tissue surface to create lesions on the heart muscle, but the only contact is not enough to generate an ablation lesion. Pushing a catheter to achieve contact with tissue exerts a force on the tissue it is essential to facilitate efficient heat energy transfer to a target tissue. Thus, the effects of catheter contact force in creating effective lesions and its part of the ultimate success of a radiofrequency catheter cardiac ablation procedure. Moreover, contact force imparted on heart tissue linked to the potential for complications such as cardiac perforation, steam pop, and thrombus formation. It is also linked to collateral tissue damage to the heart's structure, such as oesophageal, pulmonary, and phrenic nerve injury [30, 39, 44, 63].

2.4 SUMMARY

RF catheter ablation has rapidly emerged as the effective minimally invasive treatment of choice for some cardiac arrhythmias. Catheter contact force and contact angle play an important role in RF ablation lesion formation. In addition, contact force imparted on heart tissue linked to the potential for various complications. However, the effects of catheter contact force-related contact angle still have more detail that requires further elucidation in many details to fulfill the knowledge in this research field.

Chapter 3: Effects of Catheter Contact Force and Angle on Contact Area

This chapter focused on investigates the effects of catheter contact force and contact angle on the catheter contact area. The topic is this chapter are including; Section 3.1 purpose of the study, Section 3.2 methods, Section 3.3 results, Section 3.4 discussion, Section 3.5 major findings, Section 3.6 clinical implications, Section 3.7 study limitations, and Section 3.8 Conclusion.

3.1 PURPOSE OF THE STUDY

The purpose of this study was to develop an experimental procedure for setting the catheter angle with respect to the surface of the heart muscle and the catheter contact force, as well as to investigate the catheter contact area on the heart muscle as a function of catheter contact angle and contact force.

3.2 METHODS

3.2.1 Heart muscle surface flattener and preparation

Most of the surface of the heart is round, and the state of catheter contact would vary according to clinical conditions. Therefore, to provide better reproducibility of this in vitro experiments, A special instrument was developed that precisely adjusts the catheter angle between the catheter tip and the heart muscle. The instrument consists of a heart muscle surface flattener and catheter tip angle setter. As part of the heart muscle surface flattener, a circular crystalline acrylic plate with a thickness of 12 mm and a diameter of 130 mm was used to flatten the surface of porcine heart tissue and fix its position at a specific location and orientation, ensuring that all experiments using this plate will maintain uniformity, as shown in Figure 7.

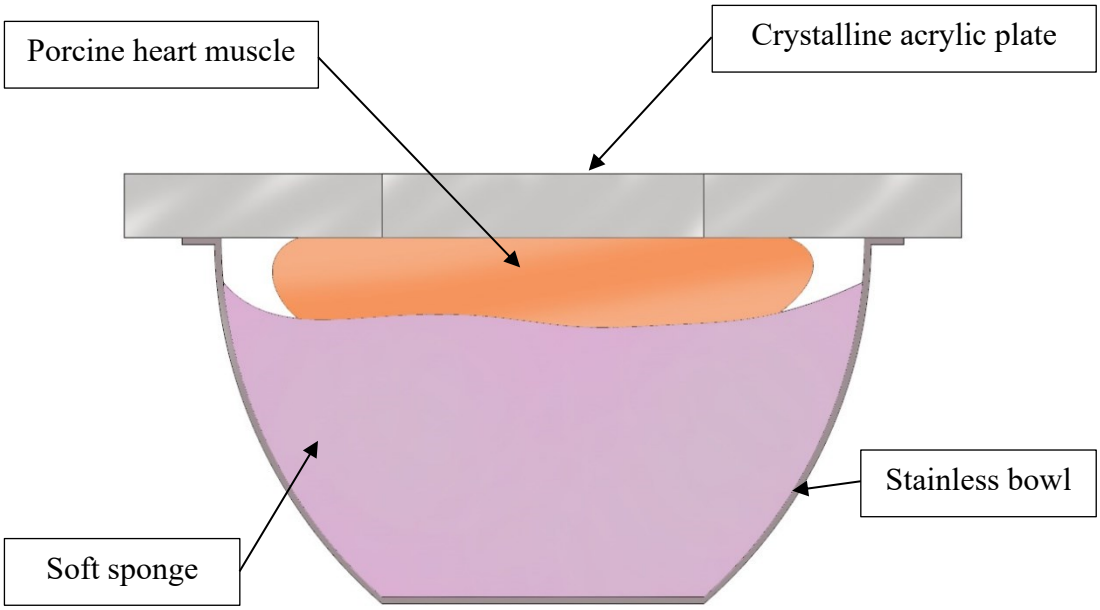

Figure 7. The heart muscle tissue is sandwiched between a flat acrylic plate and a soft sponge, which are placed in a stainless bowl, and the surface of the heart muscle was flattened by adjusting the amount of the sponge in the bottom of the bowl.

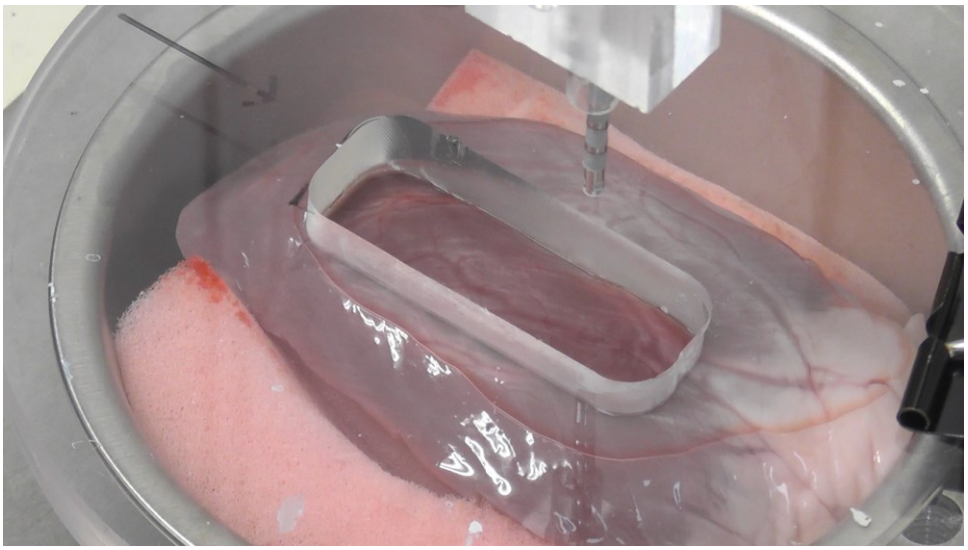

Figure 8. The surface of a portion of epicardium lacking adipose tissue was flattened.

A fresh porcine heart was obtained from a slaughterhouse at 24–48 h after animal sacrifice. A section of the ventricular myocardium was cut into 20–30-mm-thick pieces, and kept at room temperature in a closed container under moist conditions to prevent drying. Before the experiment, the pieces were removed from the closed container and sandwiched between the acrylic plate and a soft sponge placed in a

stainless bowl. The surface of a portion of epicardium lacking adipose tissue was flattened by adjusting the amount of the sponge. The catheter ablation experiments were performed through a hole (20 mm × 50 mm) in the acrylic plate, as shown in Figure 8.

3.2.2 Catheter's description

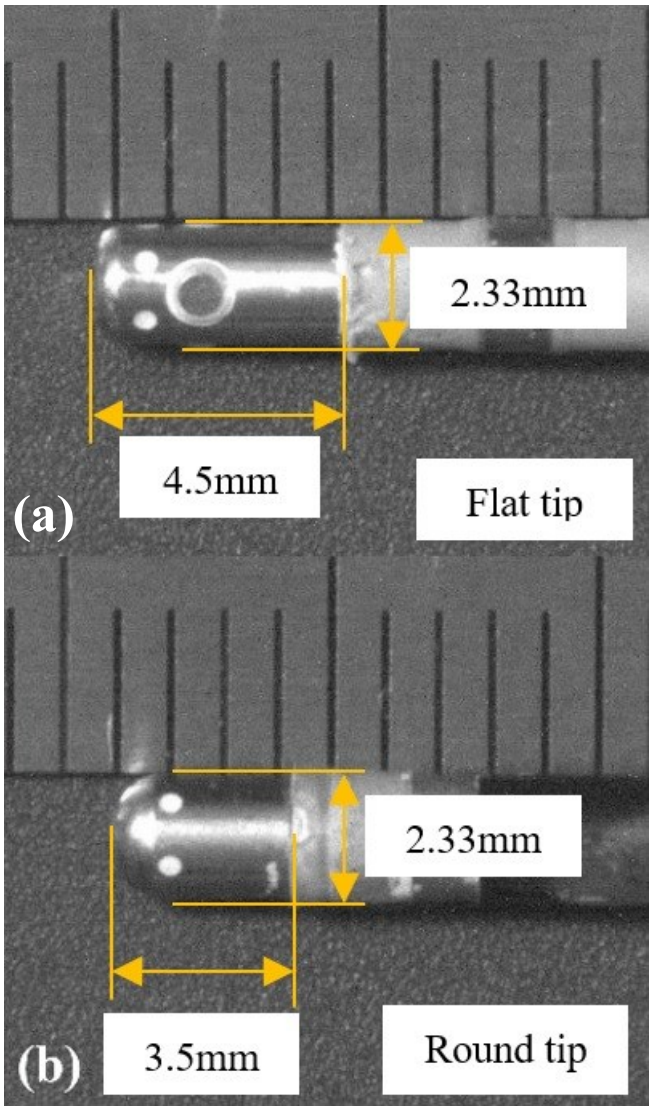

Figure 9. open-loop irrigated catheter; **(a)** IntellaNav Mifi™ catheter-tip electrode. **(b)** Abbott TactiCath™ dcatheter-tip electrode.

Two different open-loop irrigated catheter tips were used in this study (Figure 1b). One was the IntellaNav Mifi™ open-loop irrigated catheter tip (7 Fr/4.5 mm 7.5 Fr; PMR9620, Boston Scientific Inc.), as shown in Figure 9 (a). The catheter was 110 cm long, with a tip length of 4.5 mm, and had a standard curve style. The catheter incorporates an open-loop irrigated cooling mechanism through the tip and is partitioned into two chambers.

The other catheter was an Abbott TactiCath™ (7 Fr/3.5 mm 7.5 Fr; Quadripolar, PN-004075, St. Jude Medical, Inc.), as shown in Figure 9 (b) which is representative of round-tip catheters. It was 115 cm long, with a tip length of 3.5 mm, and had a steerable curve style. Both catheters were open-loop irrigated catheters, with 6 small irrigation holes circumferentially located on the lateral surface of the tip. Irrigation of the catheter tip was designed to reduce excessive heating of the tissue and blood at the catheter tip. The main difference between the two catheters is the shape of the end tip.

3.2.3 Contact area visualization experimental system incorporating the catheter angle setter and contact force sensor

To elucidate the effects of the catheter contact angle and contact force on the contact area of the heart tissue surface, A special experimental procedure was developed that enables the setting of various catheter contact angles (0, 30, 45, 60, and 90 degrees) using a special acrylic tube guide, as well as the measurement of the contact force. In the experimental setup, a digital force sensor (FGP-0.5, Nidec-Shimpo Corporation) was mounted on a motion stage (FGS-5000TV, Nidec-Shimpo Corporation), the position of which can be controlled vertically. Using this setup, the catheter contact force and contact angle could be precisely controlled. The system was operated using commercial software (FGT-TV) running on a computer, as shown in Figure 10.

White soluble ink (Pen Cure, Japan Pen Company) was overlaid on the metal electrode of the catheter tip to visualize the contacted area on the heart tissue surface, as shown in Figure 11. Then, the 8 levels of contact force within the clinically used

range; (2, 4, 6, 10, 15, 20, 30, and 40 gf) were applied to the cardiac muscle in line with the typical clinical contact force ranges [56–58]. Using this process, the catheter contact area-visualization test was repeated 6 times each for the 5 contact angles and 8 contact forces to ensure equal distribution of contact force. In the final step, all of the catheter contact areas for each condition were photographed for the evaluation of contact area through image analysis.

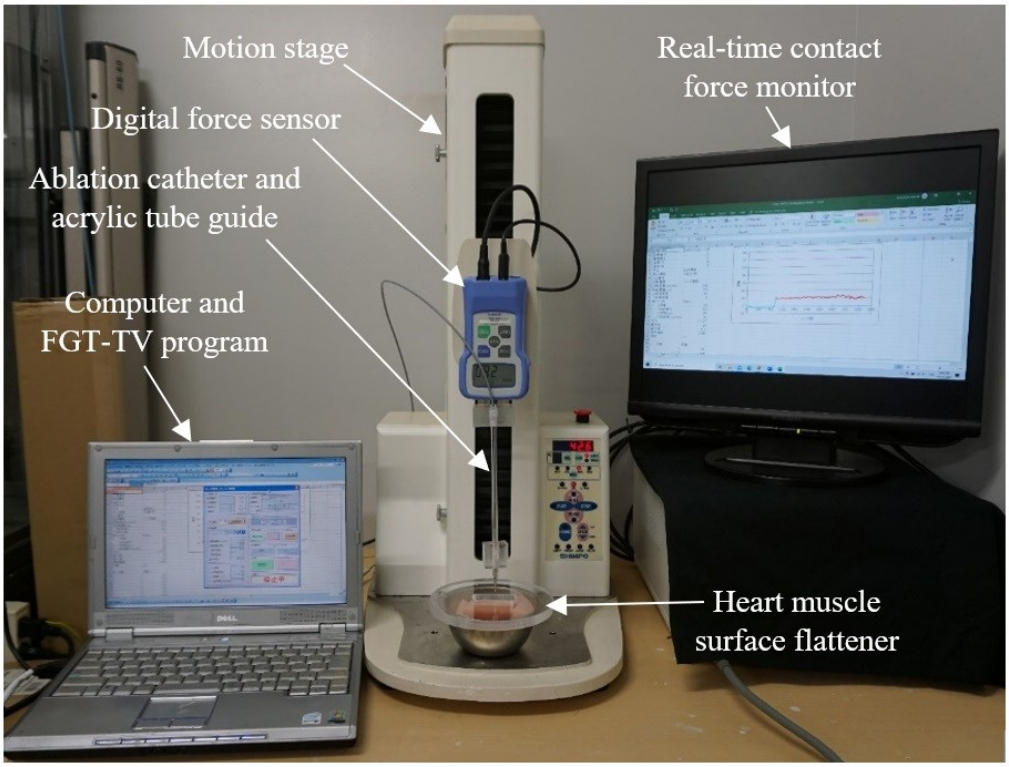

Figure 10. Experimental setup. A compact desktop test stand equipped with a digital force gauge was controlled using an FGT-TV software link from a computer. In this picture, the acrylic tube guide for 90 degrees was used.

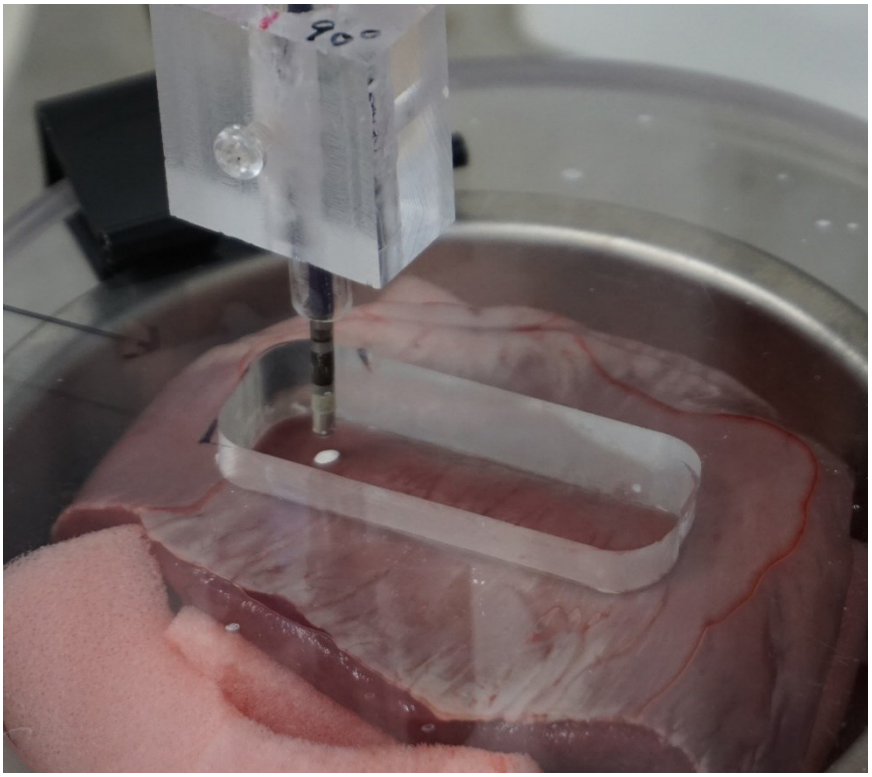

Figure 11. White soluble ink was overlaid on the metal electrode of the catheter tip to visualize the contacted area on the heart tissue surface.

3.2.4 Contact area visualization evaluation

As shown in Figure 12., image analysis of photographs of the catheter contact area was performed to evaluate the morphology of the contact area. The image analysis program MATLAB (Version 2019a) was used to perform the following actions, as shown in Figure 9. First, the raw colour image of the contact area was manually segmented into individual lesion images and converted into a grayscale image, and finally the grayscale image was binarized. Next, the catheter contact area on the heart tissue surface was calculated. To understand the morphology of the contact area, the centroid of each contact area image was aligned to create a reference point for comparison. Then, the image was rotated about the centroid to align each area's longest axis parallel to the vertical direction. The average morphology of the contact area was derived from 6 experimentally acquired images. The morphological characteristics corresponding to physical parameters were also evaluated. All statistical analyses were performed using GraphPad Prism software (Version 8.4.3).

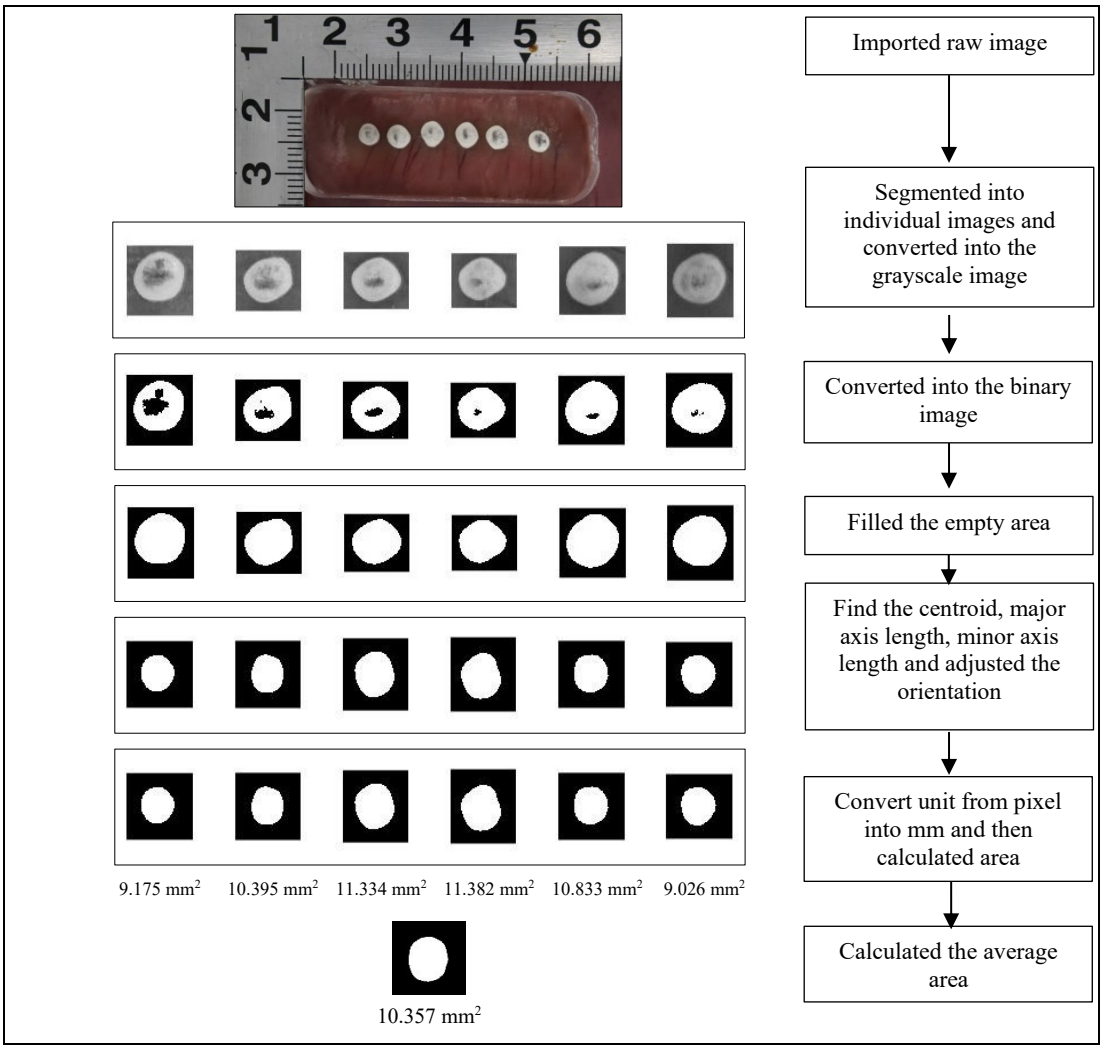

Figure 12. Chart of the flow process for evaluating the morphology of the contact area and the average contact area at a contact angle of 90 degrees and a contact force of 30 gf using a round-tip catheter.

3.3 RESULTS

3.3.1 Verification of catheter-tissue contact force

For validation of the experimental system, a fixed loading force of 10 gf was applied to the cardiac muscle. Then, all parameters were controlled by FGT-TV software. The control parameters are assigned in this experiment are shown in Table 1. Using this process, the experiments were tested 5 times each for the 5 contact angles and repeated 6 times at each contact angle.

Figure 13. show the visualized contact area and the generated ablated area under such a corresponding condition. Figure 14. (a) – (e) shows the estimated values of 6 contact areas for the 5 contact angles among 0, 30, 45, 60 and 90 degrees, respectively. Table 2 shows the contact area data, those averaged data, those standard deviations, and those coefficients of variation.

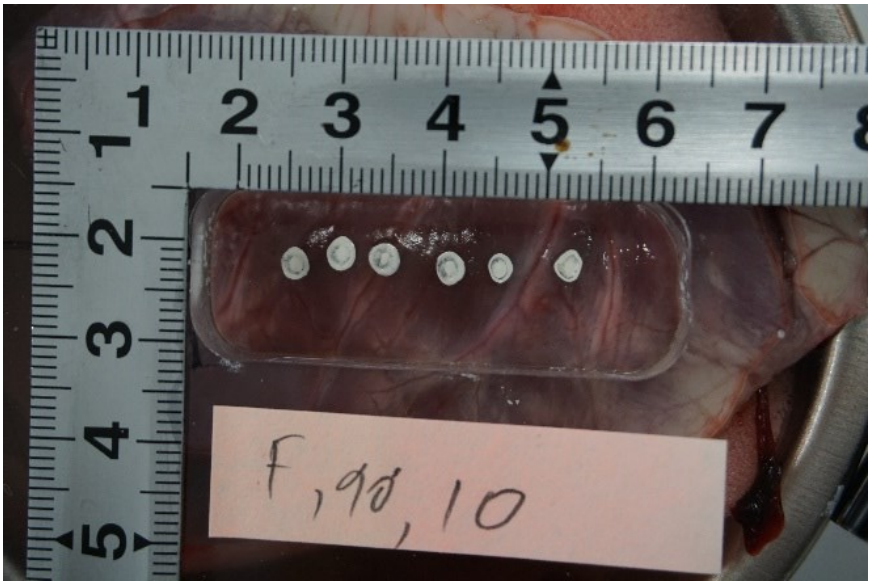

Figure 13. The visualized contact area at 90-degree contact angle.

Table 1. Control parameters of motion stage.

Parameter		Unit
Test speed	10	mm/min
Travelled Distance	50	mm
Contact force	10	gf
Upper limit load	50	gf
Lower limit load	0	gf
Contacting time	30	sec
Pre-contacting speed	5	mm/min
Recording cycle	100	time/sec

Table 2. Catheter contact area[mm^2], those averaged value, those standard deviation, and those coefficients of variation.

Contact angle (deg)					
Test#	0	30	45	60	90
1	13.83	11.45	10.04	10.37	6.41
2	15.13	10.09	9.23	10.09	5.39
3	14.83	8.42	10.00	9.15	7.37
4	15.30	9.97	10.93	8.83	7.75
5	12.64	7.87	10.82	10.09	7.50
6	12.51	9.83	11.74	8.46	6.85
AVG.	14.04	9.61	10.46	10.09	6.88
S.D.	1.24	1.28	0.88	0.79	0.87
C.V.	8.86%	13.36%	8.43%	8.29%	12.71%

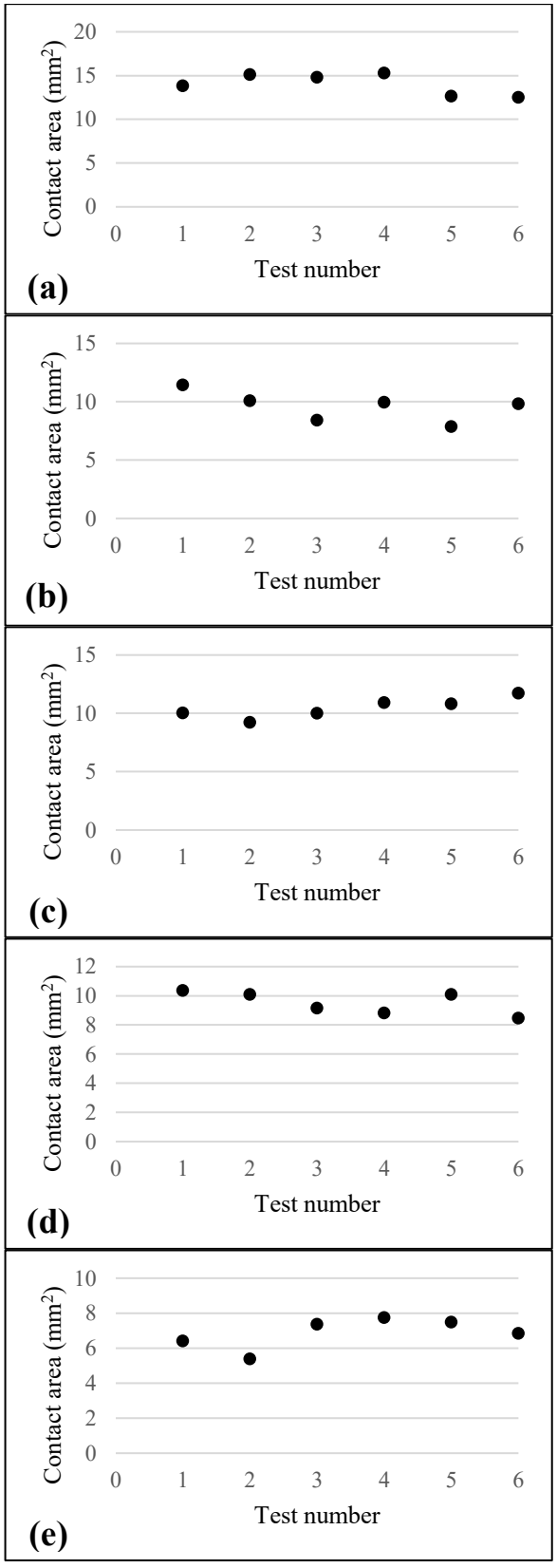

Figure 14. The contact area at a catheter contact angle of **(a)** 0 deg, **(b)** 30 deg, **(c)** 45 deg, **(d)** 60 deg, and **(e)** 90 deg.

3.3.2 Contact area morphology

Figure 15 shows the four distinct morphologies of the contact area with a contact angle of 0 degrees using the flat-tip catheter and contact angles of 0, 30, and 90 degrees using the round-tip catheter. These images show that the contact angle and shape of the catheter tip can affect the contact area morphology. For example, the morphology differs according to the shape of the catheter tip, even when both are applied at a contact force of 2 gf and a contact angle at 0 degrees. In contrast, the morphology was similar when both shapes were applied at a contact force of 2 gf and a contact angle at 90. Further details about the differences in contact area morphology will be discussed later in the Discussion section.

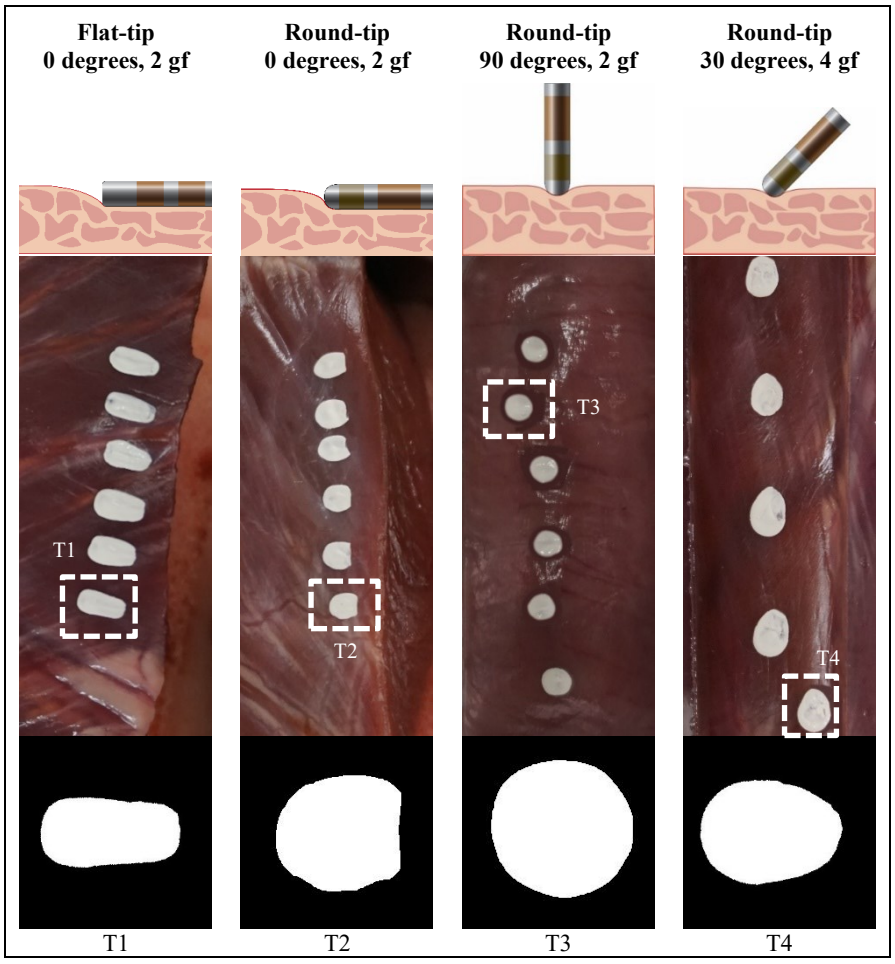

Figure 15. Morphology of the contact area on a porcine heart under various contact conditions. T1–T4 represent the morphology of the four types of contact area.

3.3.3 Average contact area

Data of average contact areas, standard deviations, and percentage of contact area for flat-tip and round-tip catheters are shown in Tables 3 and 4, respectively. The ratio of the area of the catheter in contact with heart muscle to the catheter tip surface area was calculated by the following equation:

$$Percentage\ contact\ area\ = \left(\frac{Catheter/heart\ contact\ area}{Catheter\ tip\ surface\ area}\right) \times 100$$

where the catheter tip surface area of the flat-tip catheter is 37.26 mm^2 and that of the round-tip catheter is 25.67 mm^2.

The standard SI unit for force is the newton (N), but gram-force (gf) is frequently used to measure contact force in the field of catheter ablation research (1 gf = 0.00981 N, which is the force acting on a mass of 1 g under the Earth's gravitational acceleration of 9.81 m/s^2). The contact forces tested in this study were 2, 4, 6, 10, 15, 20, 30, and 40 gf, which correspond to 0.0196, 0.0392, 0.0588, 0.098, 0.147, 0.196, 0.294, and 0.392 N, respectively.

Table 3. Average contact area and percentage contact area when using the flat-tip catheter (mm^2)

Contact angle	Contact force (gf)											
	2			4			6			10		
	AVG CA	SD	PCA (%)	AVG CA	SD	PCA (%)	AVG CA	SD	PCA (%)	AVG CA	SD	PCA (%)
0 deg	11.424	1.123	31%	10.861	1.188	29%	10.547	1.079	28%	14.041	1.245	38%
30 deg	6.002	0.908	16%	7.406	0.594	20%	7.941	1.625	21%	9.607	1.284	26%
45 deg	7.058	0.928	19%	7.027	0.608	19%	10.199	0.873	27%	10.463	0.883	28%
60 deg	4.641	0.605	12%	7.247	1.228	19%	8.163	1.791	22%	10.094	1.996	27%
90 deg	3.445	0.831	9%	4.392	0.514	12%	5.627	0.555	15%	6.879	0.874	18%
Contact angle	**Contact force (gf)**											
	15			**20**			**30**			**40**		
	AVG CA	SD	PCA (%)	AVG CA	SD	PCA (%)	AVG CA	SD	PCA (%)	AVG CA	SD	PCA (%)
0 deg	15.458	1.392	41%	15.358	1.624	41%	16.405	1.050	44%	19.097	1.294	51%
30 deg	13.178	2.103	35%	14.644	2.609	39%	11.769	1.914	32%	14.759	1.196	40%
45 deg	11.820	0.680	32%	12.842	1.438	34%	14.860	1.672	40%	19.533	1.361	52%
60 deg	11.131	1.590	30%	11.431	1.699	31%	12.114	1.443	33%	13.515	0.895	36%
90 deg	8.363	0.982	22%	7.405	1.126	20%	9.508	1.040	26%	12.589	0.812	34%

AVG CA, average contact area; SD, standard deviation; PCA, percentage contact area

Table 4. Average contact area and percentage contact area when using the round-tip catheter (mm^2)

Contact angle	Contact force (gf)											
	2			4			6			10		
	AVG CA	SD	PCA (%)	AVG CA	SD	PCA (%)	AVG CA	SD	PCA (%)	AVG CA	SD	PCA (%)
0 deg	6.365	0.508	25%	8.730	0.840	34%	9.039	1.040	35%	10.325	1.159	40%
30 deg	6.055	1.075	24%	6.999	0.825	27%	9.982	0.768	39%	12.579	1.107	49%
45 deg	3.592	0.493	14%	4.906	0.421	19%	5.547	0.629	22%	6.815	0.898	27%
60 deg	3.699	0.724	14%	5.869	0.719	23%	6.782	0.821	26%	8.222	0.625	32%
90 deg	3.829	0.294	15%	6.309	0.320	25%	7.797	1.134	30%	7.990	0.553	31%
Contact angle	**Contact force (gf)**											
	15			**20**			**30**			**40**		
	AVG CA	SD	PCA (%)	AVG CA	SD	PCA (%)	AVG CA	SD	PCA (%)	AVG CA	SD	PCA (%)
0 deg	11.779	1.292	46%	12.343	1.042	48%	13.661	0.852	53%	15.578	1.274	61%
30 deg	14.417	2.141	56%	13.697	1.857	53%	17.693	1.394	65%	16.788	0.581	65%
45 deg	8.123	0.652	32%	9.704	0.841	38%	12.730	1.583	50%	13.725	1.954	53%
60 deg	9.354	0.811	36%	10.275	0.868	40%	10.464	1.740	41%	14.310	2.286	56%
90 deg	8.535	0.751	33%	9.340	0.638	36%	10.357	1.039	40%	11.914	0.909	46%

AVG CA, average contact area; SD, standard deviation; PCA, percentage contact area

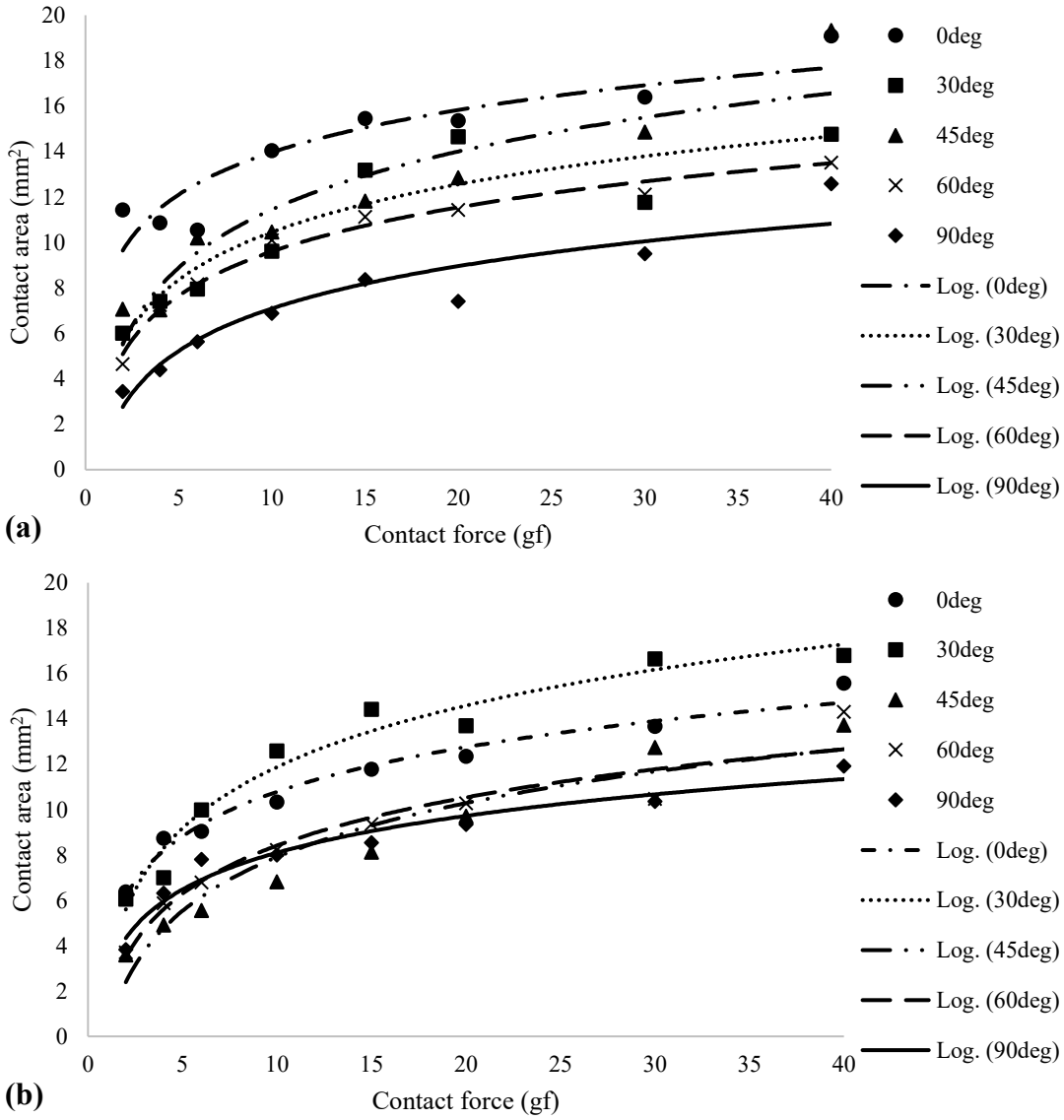

Figure 16. Plot of average contact area and contact force for **(a)** flat-tip catheters and **(b)** round-tip catheters at each contact angle.

Figure 16 (a) and (b) shows a plot of the catheter contact areas created with the contact forces on the x-axis and the contact area on the y-axis for both catheter shapes. This plot illustrates the correlation between contact force, contact angle, and contact area. The results revealed a positive correlation between contact force and contact area, in which increased contact force was associated with increased contact area. Moreover, the contact angle had as strong an effect on the contact area as the contact force did. At the same contact force, the correlation between contact angle and contact area was inverse; that is, a smaller contact angle was associated with an increased contact area. The logarithmic approximation formulas for expressing the relationship between

contact area and contact force for each catheter contact angle are shown in Table 5. The data reveal that the correlation between contact force and the contact area is a logarithmic function with R-Squared (R^2) being nearly equal to 1.

Figure 17 shows binarized images of the average contact areas under the various conditions (8 contact forces and 5 contact angles) when using the flat-tip and round-tip catheters. These data clearly show that the contact angle had as much influence as the contact force on the contact area. For example, using the flat-tip catheter at a contact angle of 90 degrees, the contact force increased from 2 to 4, 6, 10, 15, 20, 30, and 40 gf, and the average contact area increased from 3.445 to 4.392, 5.627, 6.879, 8.363, 7.405, 9.508, and 12.589 mm^2, respectively. In addition, using the round-tip catheter at a contact angle of 90 degrees, the contact force increased from 2 to 4, 6, 10, 15, 20, 30, and 40 gf, and the average contact area increased from 3.829 to 6.309, 7.797, 7.990, 8.535, 9.340, 10.357, and 11.914 mm^2, respectively. Similar trends were seen for both shapes of catheters at contact angles of 60, 45, 30, and 0 degrees.

Table 5. Approximation formulas expressing the relationship between catheter contact area and contact force for each catheter contact angle, where x is catheter contact force (gf), y is catheter contact area (mm^2), and R^2 is coefficient of determination, respectively.

Angle (degree)	Flat-tip		Round-tip	
	Approximation formula	R^2	Approximation formula	R^2
0	y = 2.685ln(x) + 7.782	0.837	y = 2.837ln(x) + 4.251	0.974
30	y = 3.036ln(x) + 3.465	0.845	y = 3.903ln(x) + 2.890	0.961
45	y = 3.689ln(x) + 2.952	0.867	y = 3.429ln(x) + 0.012	0.926
60	y = 2.807ln(x) + 3.137	0.984	y = 3.062ln(x) + 1.363	0.936
90	y = 2.693ln(x) + 0.892	0.893	y = 2.341ln(x) + 2.709	0.953

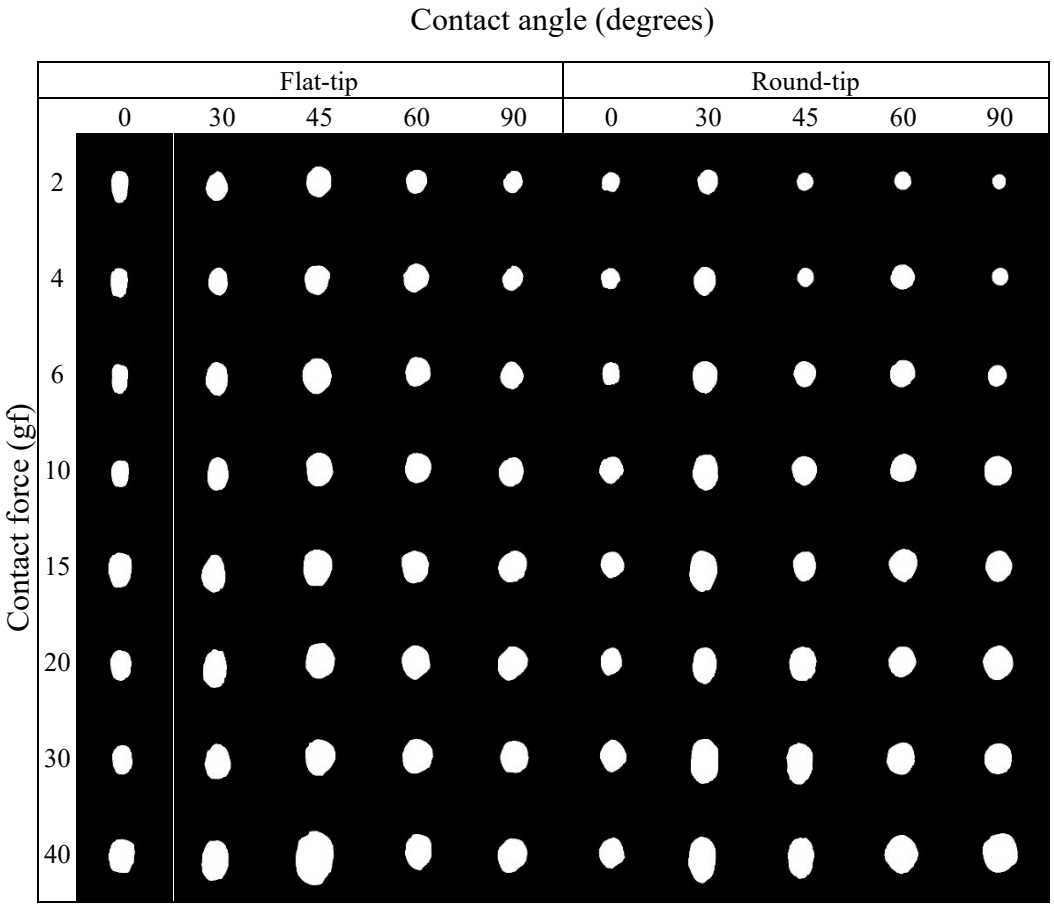

Figure 17. Average contact area morphology using flat-tip and round-tip catheters under various conditions.

3.4 DISCUSSIONS

3.4.1 Catheter contact force validation

This experimental system has flexibly adjusted the catheter contact angles among 0, 30, 45, 60, to 90 degrees between the catheter tip and the heart muscle. This system also the flexibly controlled the real-time catheter contact force. The validation test of this experimental system was performed through visualization test of the catheter contact area on the porcine heart muscle. And then, visualization tests were also performed on the ablation area under the condition with contact force of 10 gf at 90-degree. The six-contact area at such same condition about contact angle and contact force showed similar value with small standard deviations suggesting feasibility of present experimental setup. The standard deviation of contact angle 45, 60 and 90 degrees less than 1, while the standard deviation of contact angle 0 and 30

degrees approximately 1.2, as shown in Figure 18. The coefficient of variation of the contact angle, as shown in Figure 19. from 0, 30, 45, 60 and 90 are 8.86%, 13.36%, 8.43%, 8.29% and 12.71%, respectively.

From the results, the present experimental system has enough capability of setting the catheter contact angle with respect to the surface of the heart muscle and the catheter contact force. However, in order to apply this experimental system's usefully for studying radiofrequency catheter ablation, the number of tests needs to test with a more different contact force required. Especially in line with the typical clinical contact force ranges from 2 gf to 40 gf [56]. Therefore, this point needs to examine in an additional future study. This experimental system will be planned to apply to study the relationship of catheter contact angle and contact force with the contact area on the surface of heart muscle tissue in cardiac catheter ablation. Moreover, in the near future, this system will apply to investigate the lesion size as the function of the contact area, contact force and contact angle in vitro experiments.

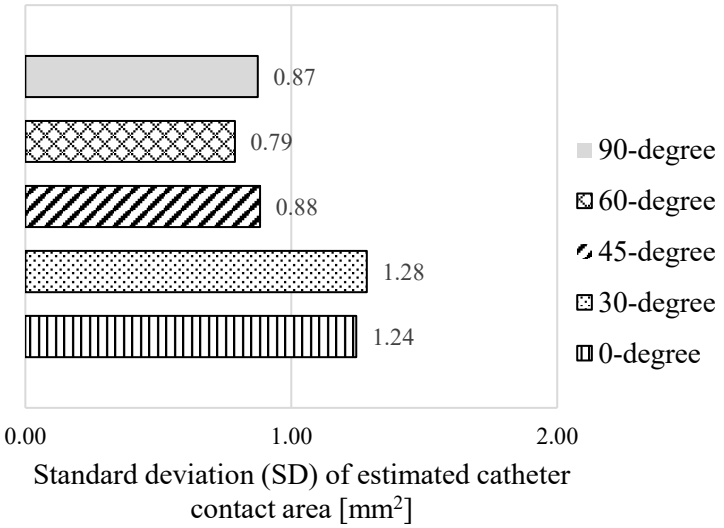

Figure 18. The standard deviation of the contact area of each catheter contact angle.

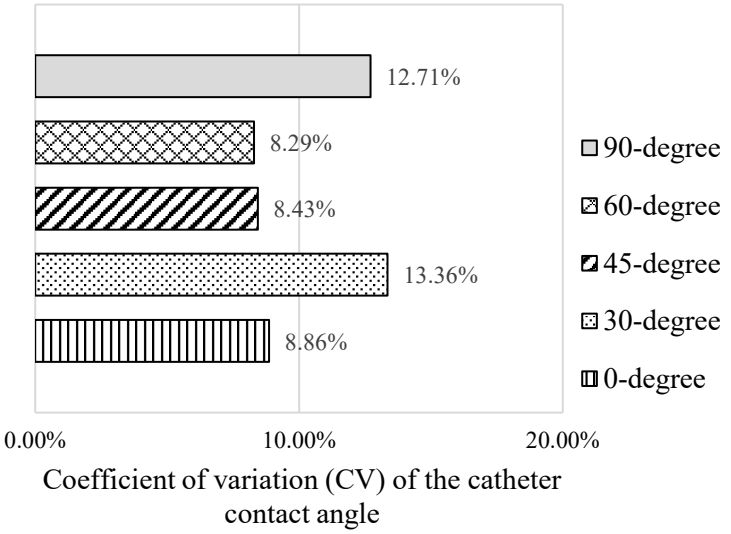

Figure 19. The coefficient of variation of the contact area of each catheter contact angle.

3.4.2 Morphological characterization of the contact area

To elucidate the effects of catheter contact angle and contact force on the contact area, we constructed a heart muscle surface flattener to maintain a flat surface to test a range of contact angles. This instrument was designed to achieve improved experimental reproducibility. Although in routine clinical ablation procedures, the surface of the heart tissue is not flat, this data clearly demonstrated that the contact angle and shape of the catheter tip substantially affected the contact area morphology. In summary, we categorized the morphology of the contact area into four types, as shown in Figure 20. A notable difference occurred when the catheter angle became parallel to the heart surface. Contact area morphology became rectangular when using a flat end tip and semi-ellipsoidal when using a round end tip. This observation clearly shows the effect of the shape of the catheter. When contact is made at a perpendicular angle, the contact area morphology is circular because the projected area of both catheters is a circle, and thus the contact area becomes circular. When the catheter is inclined, the contact area becomes ellipsoidal like an egg. Those morphological character trends changed similarly for both round- and flat-tip catheters except in the parallel (0-degree) direction.

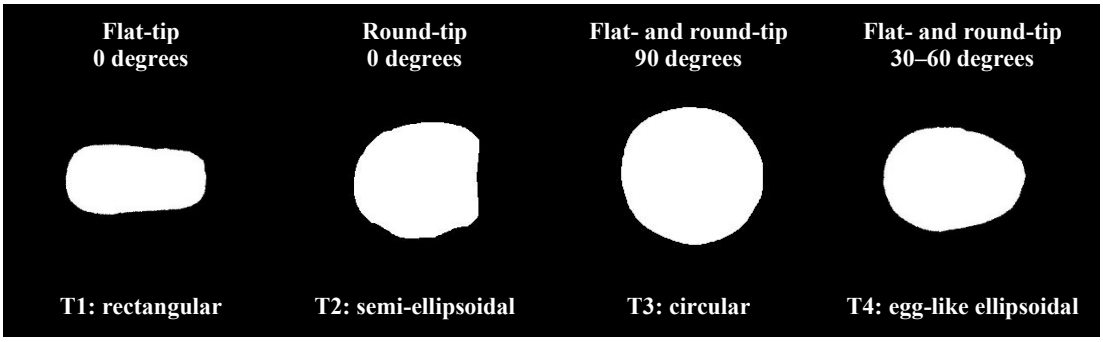

Figure 20. Contact area morphologies. The T1 morphology represents the contact area of the flat-tip catheter at a contact angle of 0 degrees. The T2 morphology represents the contact area of the round-tip catheter at a contact angle of 0 degrees. The T3 morphology represents the contact area of both the round- and flat-tip catheters at a contact angle of 90 degrees. The T4 morphology represents the contact area of both the round- and flat-tip catheters at a contact angle of between 30 and 60 degrees.

3.4.3 Correlation between contact force and contact area

Catheter contact force shows a strong positive correlation with contact area. When the contact force was increased, the contact area also increased. These results are similar to those in earlier reports [49–51, 56–58]; however, it is essential to consider the small changes in contact area that occurred at higher contact forces. The contact area increased monotonically but logarithmically. The slope of the graph changes slightly when the contact force is between 15 and 40 gf, which is in contrast to the greater change in slope when during initial contact when the contact force ranges from 2 to 15 gf. The equation for estimating contact area might help those performing this procedure to understand the relationships among the parameters and to calculate the contact area as a function of contact force at each contact angle. These data suggest a limit to the extent by which lesion size can be increased by increasing the contact force. The catheter contact angle relative to the heart muscle tissue surface can also needs to be considered when calculating the desired lesion size.

3.4.4 Correlation between contact angle and contact area

The results clearly demonstrate that the contact angle is a key determinant of the contact area morphology. In addition, the contact angle substantially affects the contact

area of the catheter tip regardless of the contact force. For the flat-tip catheter, the minimum contact area was produced at a contact angle of 90 degrees and increased with decreasing contact angle from 90 to 60, 45, 30, and 0 degrees. For the round-tip catheter, the minimum contact area was produced at a contact angle of 90 degrees and increased with decreasing contact angle from 90 to 60, 45, 0, and 30 degrees. For both catheter shapes, the contact area progressively increased when the contact angle was decreased. However, the results show a difference between the flat- and round-tip catheters at 0 and 30 degrees. These differences were due to the difference in shape and size between the two shapes of catheter tip. The two catheters used for this study were made by different manufacturers and differ in size according to their shape, especially at a contact angle between 0 and 30 degrees. The round-tip catheter makes less surface contact with the heart tissue surface compared with the flat-tip catheter. Despite this fact, the results of the experiment as a whole show a similar tendency.

3.5 MAJOR FINDINGS

The major findings are as follows: **(i)** The morphology of the contact area can be divided into four types: rectangular, circular, ellipsoidal, and semi-ellipsoidal. The morphology of the contact area indicates that **(ii)** the correlation between contact force and contact area is a logarithmic function; that is, increased contact force was associated with increased contact area, and the contact angle has as strong an effect on the contact area as contact force does. **(iii)** There is an inverse correlation between contact angle and contact area; smaller contact angle is associated with increased contact area.

3.6 CLINICAL IMPLICATIONS

Present data should be useful for those performing this procedure to understand the relation among the parameters and plan their treatment strategy beforehand. From these experiments, the contact area morphology was derived as a function between the contact angle and contact force. It is reasonable to assume that the contact area is directly related to the area of resulting lesion.

3.7 STUDY LIMITATIONS

This study has several limitations. First, we aimed to test the assumptions about contact angle, contact force, and contact area by using two different shapes of commercially available catheter tips. The two catheters were made by different manufacturers, and thus have some differences in design. Accordingly, we did not compare the differences in results between the catheters. Second, to provide better reproducibility of this in vitro experiments, we developed a special instrument that precisely adjusts the catheter angle between the catheter tip and the heart muscle. The instrument consists of a heart muscle surface flattener and a catheter-tip-angle setter. In clinical practice the shape of the heart tissue surface varies according to the part of the heart, and thus the catheter tip orientation can rarely be optimized due to restricting structures such as trabeculated muscle, valves, or the papillary muscle. Nevertheless, at the present stage of research on catheter ablation (pre-clinical experiment studies), it necessary to perform tests on flat surfaces to clearly demonstrate the specific effects of the catheter contact angle and contact force on the contact area of the heart tissue surface. Lastly, to produce effective ablation lesions, the depth of the lesion is at least as important as the ablation size. In this study, we did not investigate whether the catheter contact angle and contact force affected the depth of the ablation lesion; however, we conducted experiments to elucidate the effect of the catheter contact angle and contact force on the contact area. These findings might be validated in the near future through numerical simulations such as the Finite Elemental Method, which can be used to estimate cardio-muscular deformation in response to catheter tip contact or a practical investigation through an in vitro heart muscle ablation experiment.

3.8 CONCLUSION

This study clearly demonstrated a substantial impact of the contact angle and contact force of a catheter on the size and morphology of the contact area in catheter ablation procedures. The contact area should be directly related to the lesion area. These data may help doctors understand the relationships among contact angle, contact

force, and contact area in ablation therapy procedures. Such information should help doctors plan appropriate treatment strategies in consideration of each patient's conditions.

Chapter 4: Effects of Catheter Contact Force and Angle on Lesion Size

This chapter investigates the effects of catheter contact force and angle on the ablation lesion dimension, ablation impedance, and their relationship. The topic is this chapter are including; Section 4.1 purpose of the study, Section 4.2 methods, Section 4.3 results, Section 4.4 discussion, Section 4.5 major findings, Section 4.6 clinical implications, Section 4.7 study limitations, and Section 4.8 Conclusion.

4.1 PURPOSE OF THE STUDY

This study aimed first to investigate the effect of catheter contact force and contact angle on the ablation lesion dimension. Second, investigate the effects of the catheter contact force related to the contact angle on the ablation impedance. Last, investigate the relationship between the catheter contact area and the dimensions of the ablation lesion as a function of catheter contact angle and force in the radiofrequency catheter ablation process.

4.2 METHODS

4.2.1 RF ablation system incorporating the catheter angle setter and contact force sensor

As shown in Figure 21., a piece of porcine heart prepared using the surface flattener was submerged in a tank containing 0.9 wt% saline and the position of the piece was fixed to the bottom of the tank. The position was set by aligning a hole in the acrylic plate with the position of the catheter. The saline tank is equipped with a motion stage having a length of 32 cm, a width of 22 cm, and base that is raised 3 cm from the floor. An anti-slip cover was also installed at the base of the tank. Holes were drilled in two sides of the saline tank to allow for the connection of dispersive electrodes with a screw and a leakproof rubber fitting to provide the return path for the RF current. In the experimental ablation setup, the saline tank was equipped with a

motion stage (FGS-5000TV, Nidec-Shimpo Corporation) on which a digital force sensor (FGP-0.5, Nidec-Shimpo Corporation) was mounted. The temperature of the saline solution was maintained at 35°C to 37°C and continuously monitored using a temperature controller (JTA-550, As One Corporation). Circulation flow in the saline-filled chamber was generated by a water pump (AD20P-0510A, DollaTek) to mimic blood flow and distribute temperature.

As shown in Figure 22., an RF ablation device (Maestro 4000, Boston Scientific Inc.) was used in this study. Saline irrigation with 0.9 wt% was performed using an irrigation pump (MetriQ, Boston Scientific Inc.) that was connected to the catheter. The IntellaNav Mifi™ open-loop irrigated catheter tip (7 Fr/4.5 mm 7.5 Fr; PMR9620, Boston Scientific Inc.) was used in this study (Figure 23 (a)). The catheter was 110 cm long, with a tip length of 4.5 mm, and had a standard curve style. The catheter incorporates an open-loop irrigated cooling mechanism through the tip and is partitioned into two chambers. The proximal chamber circulates normal saline within the tip of the cooling mechanism at the proximal end of the tip electrode and mitigates overheating while the distal chamber allows the fluid to flow through six irrigation holes into the patient's vasculature, thereby cooling the tip electrode of the ablation catheter as well as the heart tissue surface. A fluid fitting is used to make leak-free connections and connect the irrigation tubing set at the handle’s proximal end, allowing the irrigation pump to generate a flow of saline to the catheter. The electrode comprises a tip electrode and three-ring electrodes and includes three diagnostic mini-electrodes embedded in the tip, as shown in Figure 23 (b). The catheter-tip electrode has an embedded temperature sensor and delivers the RF energy for cardiac ablation.

The system was operated and monitored using FGT-TV software (Nidec-Shimpo Corporation) running on a personal computer. To investigate the effects of the catheter contact angle and contact force on the ablation dimensions of the heart tissue, we used a procedure that we developed to enable the setting of various catheter contact angles (0, 30, 45, 60, and 90 deg) using a special acrylic tube guide. To set the angle, the

catheter was inserted into the tube guide, and the tube guide was locked by turning a screw in the acrylic block mounted on the digital force gauge. The distance between the end-tip of the catheter and the end of the tube guide was fixed by turning the screw.

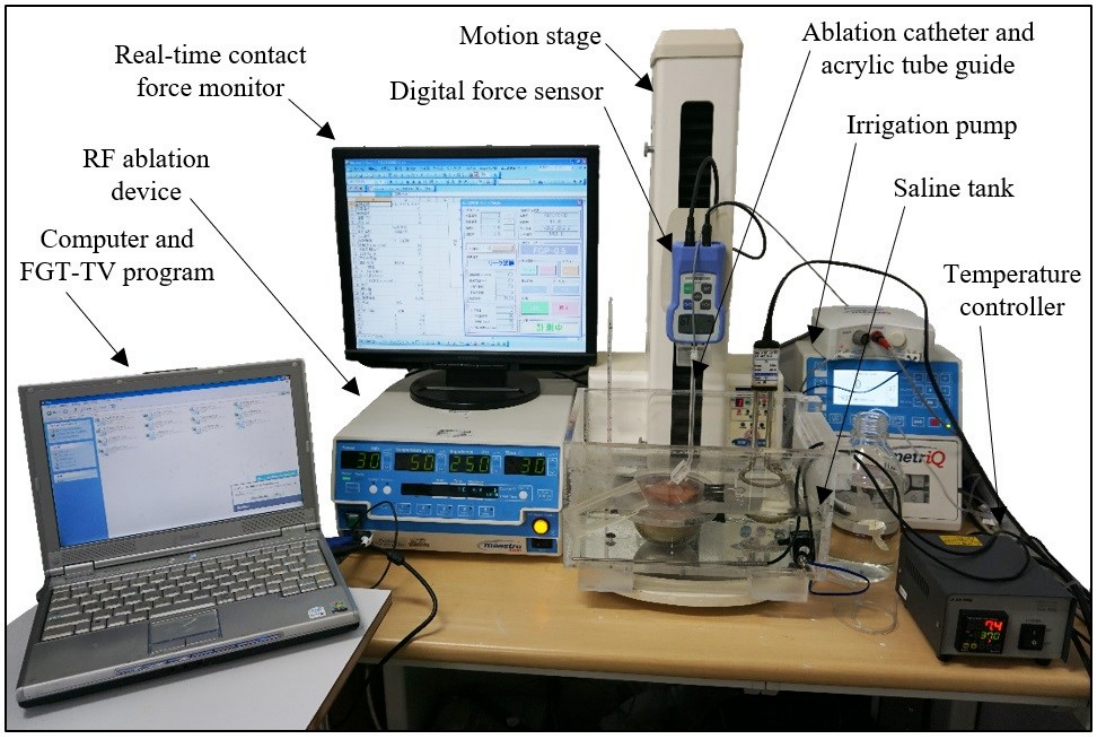

Figure 21. RF experimental setup. The saline tank was installed on a compact desktop test stand and equipped with a digital force gauge. The RF ablation device and an irrigation pump were connected to the catheter. The system was operated and monitored using FGT-TV software running on a personal computer.

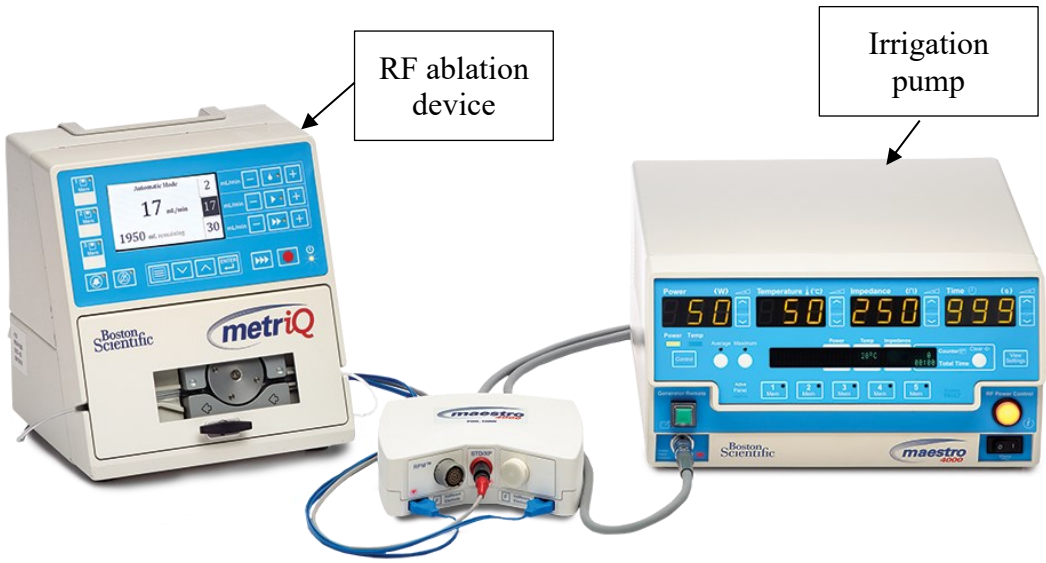

Figure 22. Cardiac Ablation System (Boston Scientific Inc.). Taken from: https://www.bostonscientific.com/en-EU/products/cardiac-ablation-systems.html

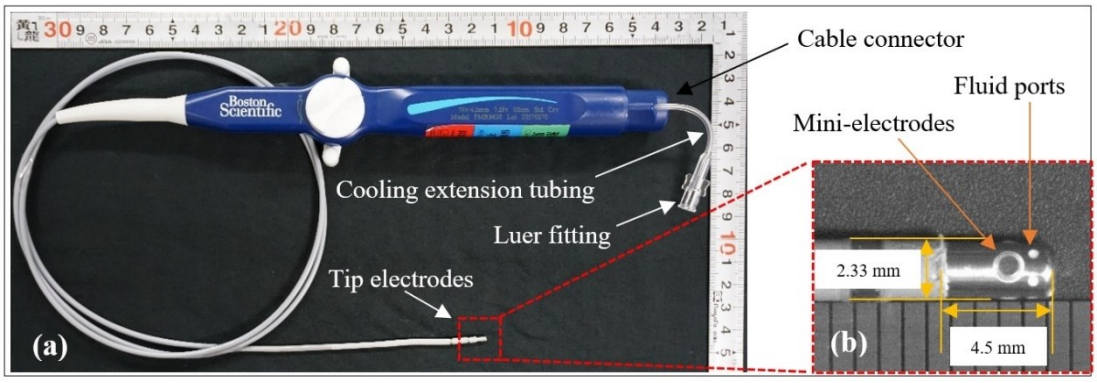

Figure 23. (a) IntellaNav Mifi™ open-loop irrigated catheter. **(b)** catheter-tip electrode.

4.2.2 Ablation parameters

In the experiments, the 8 levels of contact force within the clinically used range (2, 4, 6, 10, 15, 20, 30, and 40 gf) were applied to the heart tissue surface in line with the typical clinical contact force ranges [56–58]. Using this process, the RF catheter ablation test was repeated 6 times each for the 5 contact angles and 8 contact forces to ensure equal distribution of contact force. The ablation time was fixed at 30 s, and the initial impedance was set at 92.5 ± 2.5 Ω. The temperature during ablation was set at 30°C, and the power at 30 W. Initially, and before every ablation test, the catheter was

placed in the saline tank, where it floated, and an irrigation rate of 2 mL/min (contact force = 0 gf) was set. During ablation, the rate of irrigation with 0.9 wt% saline was subsequently increased from 2 to 17 mL/min [35, 39]. All ablation parameters are shown in Table 6. In the final step, all of the ablation lesion dimensions for each condition were photographed for later evaluation of the ablation lesion dimensions through image analysis. In total, 240 experiments (40 sets of 6 experiments each) were performed.

Table 6. Ablation parameters

Parameters	
Ablation time, s	30
Power, W	30
Initial impedance, Ω	90–95
Ablation temperature, °C	30
Saline tank temperature, °C	35–37
Initial irrigation rate, mL/min	2
Ablation irrigation rate, mL/min	17
Catheter contact force, gf	2, 4, 6, 10, 15, 20, 30, and 40
Catheter contact angle, degree	0, 30, 45, 60, and 90

4.2.3 Evaluation of ablation lesion dimensions and comparison of catheter contact area with ablation lesion area

Conventionally, ablation lesion dimensions are measured using a digital vernier caliper and the lesion area and lesion volume are calculated under the assumption that the ablation lesion is a perfectly symmetrical shape [64–66]. However, in reality, the ablation lesion morphology is never perfectly symmetrical. Moreover, the conventional method requires the investigator to visually estimate the lesion border, which is defined as the location of the change in tissue color. Measuring ablation dimensions in this way may lead to errors in ablation lesion evaluation. In the previous study (Chapter 3), we developed an experimental system for investigating the relationship of the catheter contact area on the surface of the heart tissue as a function

of catheter contact angle and force. The developed system makes possible a new technique for evaluating the catheter contact area and its morphology by using an image analysis program in MATLAB software (version 2021a; The MathWorks, Inc.). The main aim of the image analysis program was to reduce human error and improve the precision of ablation lesion evaluation. In addition, the primary purpose of the present study is to investigate the relationship between the ablation lesion area and the catheter contact area. Therefore, we used the method for evaluating lesion dimensions and the image analysis program developed in the previous study (Chapter 3), and then compared each contact area with the lesion area at the same contact condition (same force and angle).

Immediately after each set of experiments, the 6 ablation lesions were photographed using a camera (Sony A600; Lens optical 16-50mm f/3.5-5.6 OSS) with a reference scale, after which the 6 ablation lesions were bisected along their diameter and photographed again. As shown in Figure 24., the raw image with an image size 24,000,000 pixels was imported to the program and calibrated from the pixel scale to the millimeter scale. Then, the raw image was segmented into individual lesion images and converted into grayscale. The grayscale concentration level was used to define the lesion border at the pixel level, with lesion area defined as white pixels and normal tissue defined as black. In the reversible injury area, the color was not clearly white or black, so we defined the lesion area as that with a 40% concentration of white pixels. Next, each of the pixels was binarized into black or white and the empty area was filled, after which the centroid of each lesion image, the length of the minor and major axes, and lesion region area were calculated. Then, the image of each lesion was rotated about the centroid to make each area's longest axis parallel to the vertical direction. Lesion depth was measured from the top of the heart tissue surface to the maximum depth and was calculated from 6 experimentally acquired images. The average lesion area and average lesion morphology were also derived from 6 experimentally acquired images.

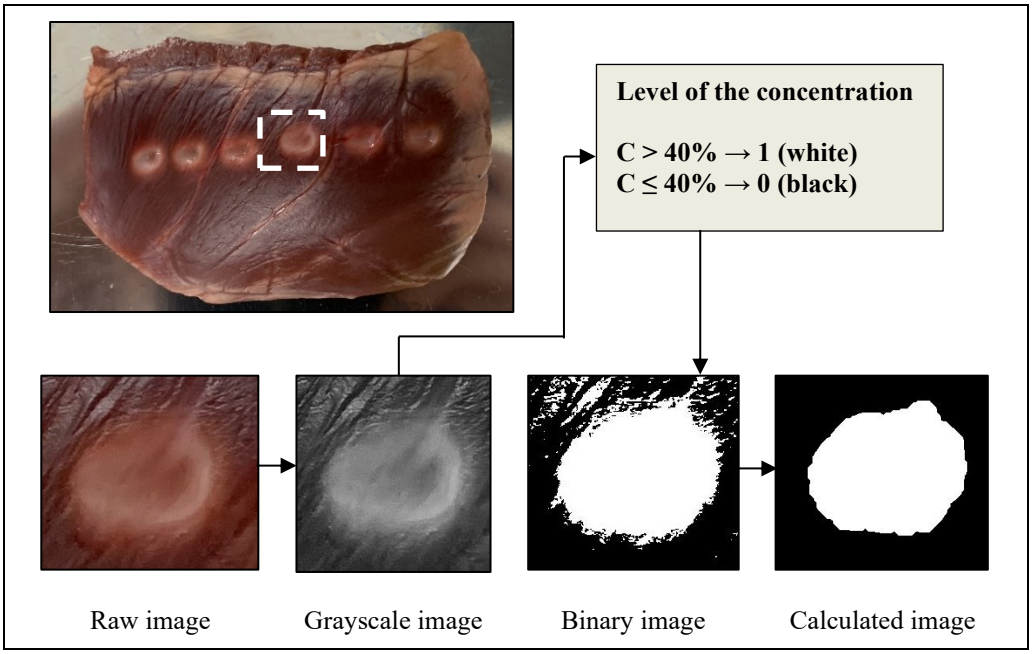

Figure 24. Image analysis process for evaluating the ablation lesion area and its morphology.

4.2.4 Statistical analysis

Pearson's coefficient (r) and Spearman's coefficient (r_s) were calculated to assess the correlation between each variable. The correlation level was described using Evans's correlation criterion. Statistical significance was defined as P-values < 0.05. Comparisons were made using Student's t-test and significant differences were defined as P-values < 0.05 (95% confidence interval). The coefficient of determination (R^2) was calculated to compare the goodness of fit of the linear and logarithmic models. All statistical analyses were performed using GraphPad Prism (version 9.0.1; GraphPad Software).

4.3 RESULTS

4.3.1 Effects of increased catheter contact force on the ablation impedance

Figure 25 shows the correlations between catheter contact force (x-axis) and maximum impedance minus average impedance (y-axis) at each contact angle. Average of maximum impedance minus average impedance at each contact angle shown in Table 7.

Table 7. Mean impedance between maximum impedance minus average impedance at each contact angle.

Contact foce	Contact angle				
	0 Deg	**30 Deg**	**45 Deg**	**60 Deg**	**90 Deg**
2 gf	9.50 Ω	10.67 Ω	13.17 Ω	13.17 Ω	12.67 Ω
4 gf	11.67 Ω	13.00 Ω	14.00 Ω	14.50 Ω	14.33 Ω
6 gf	12.33 Ω	13.83 Ω	15.17 Ω	16.00 Ω	14.50 Ω
10 gf	16.67 Ω	17.83 Ω	17.17 Ω	17.33 Ω	17.17 Ω
15 gf	18.83 Ω	18.67 Ω	19.50 Ω	18.00 Ω	21.83 Ω
20 gf	18.83 Ω	20.83 Ω	19.50 Ω	21.50 Ω	20.33 Ω
30 gf	21.00 Ω	20.33 Ω	19.33 Ω	21.00 Ω	22.50 Ω
40 gf	25.67 Ω	20.17 Ω	22.00 Ω	21.00 Ω	23.00 Ω

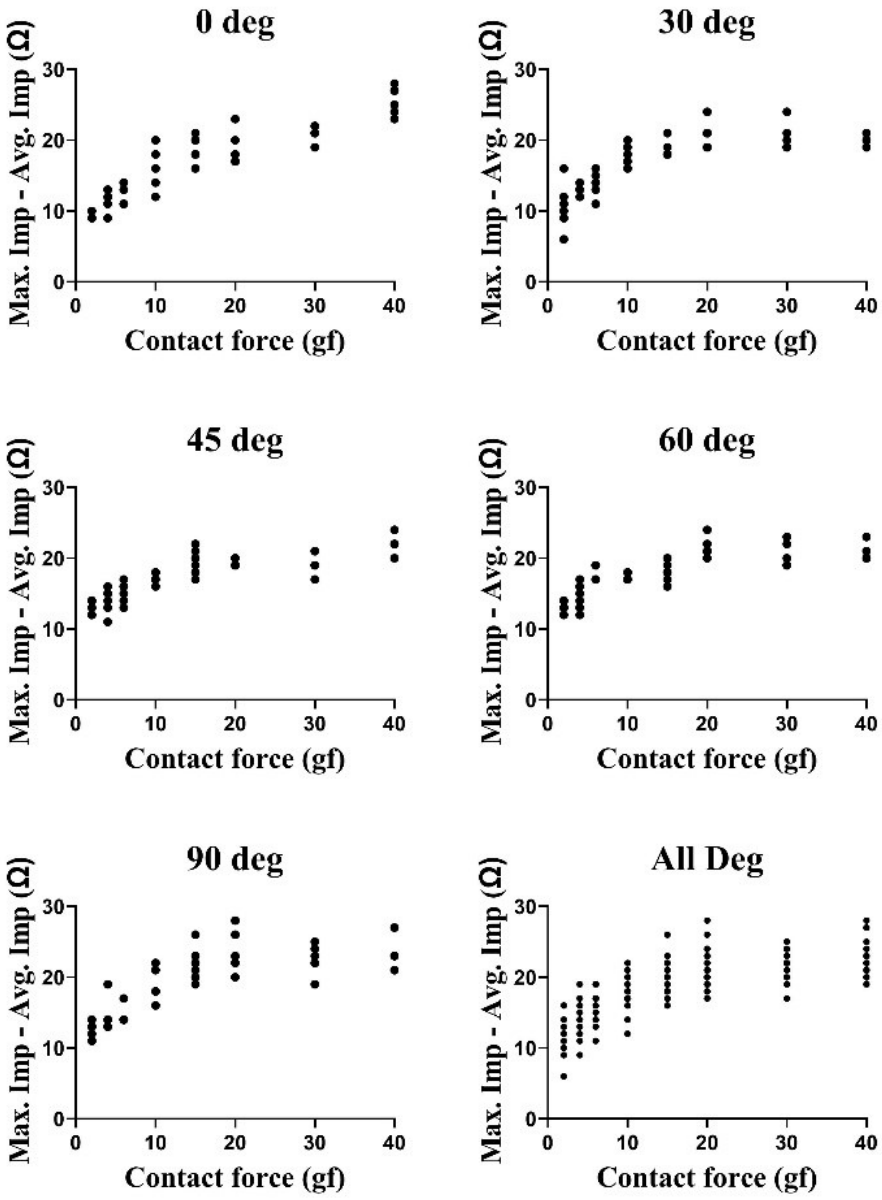

Figure 25. Correlation between catheter contact force and maximum impedance minus average impedance at each contact angle.

4.3.2 Effects of catheter contact force and angle on the ablation lesion dimension

A total of 240 lesions were ablated (40 sets of 6 experiments each); no steam pop events occurred during. The data of average lesion area and average lesion depth at each contact angle are shown as means ± SD in Tables 8 and 9, respectively. Figure 26 (a) and (b) show that not only the catheter contact force but also the catheter contact angle can affect the lesion depth and lesion area. For example, the lesion depth and

lesion area differ according to the catheter contact angle, even when the same contact force of 30 gf is applied. Further details about the relationships among catheter contact force, catheter contact angle, catheter contact area, and ablation lesion dimensions will be discussed in the following section.

Table 8. Average lesion area (mm^2)

Contact force	Contact angle				
	0 Deg	30 Deg	45 Deg	60 Deg	90 Deg
2 gf	16.67 ± 1.63	16.46 ± 3.00	12.93 ± 1.13	9.05 ± 1.79	13.28 ± 1.49
4 gf	24.17 ± 4.14	21.58 ± 2.94	19.98 ± 0.68	19.07 ± 3.43	18.53 ± 1.46
6 gf	24.05 ± 3.46	23.81 ± 1.40	19.76 ± 3.06	20.52 ± 2.23	17.09 ± 3.10
10 gf	35.54 ± 1.59	37.35 ± 3.88	21.70 ± 2.24	20.99 ± 0.79	21.89 ± 1.90
15 gf	37.81 ± 2.87	34.23 ± 3.98	24.01 ± 0.65	23.26 ± 3.55	19.55 ± 0.87
20 gf	36.10 ± 3.18	28.90 ± 6.62	32.59 ± 4.58	30.41 ± 6.69	22.78 ± 3.84
30 gf	38.04 ± 6.07	40.60 ± 6.78	35.37 ± 5.39	33.44 ± 3.79	29.85 ± 1.46
40 gf	44.10 ± 3.50	40.33 ± 6.90	39.38 ± 5.82	41.87 ± 5.68	37.62 ± 7.27

Data are shown as means ± SD.

Table 9. Average lesion depth (mm)

Contact force	Contact angle				
	0 Deg	30 Deg	45 Deg	60 Deg	90 Deg
2 gf	1.98 ± 0.30	1.70 ± 0.23	1.92 ± 0.39	2.20 ± 0.40	3.68 ± 0.38
4 gf	1.90 ± 0.14	2.02 ± 0.36	2.14 ± 0.20	2.31 ± 0.32	4.16 ± 0.47
6 gf	2.50 ± 0.32	2.23 ± 0.28	2.49 ± 0.22	3.10 ± 0.66	4.25 ± 0.33
10 gf	3.43± 0.53	3.43 ± 0.43	3.04 ± 0.45	3.80 ± 0.45	4.49 ± 0.38
15 gf	3.74 ± 0.40	3.40 ± 0.62	3.46 ± 0.77	4.76 ± 0.65	5.89 ± 0.61
20 gf	4.09 ± 0.43	4.16 ± 0.55	3.78 ± 0.54	4.45 ± 0.56	5.80 ± 0.50
30 gf	4.10 ± 0.21	4.26 ± 0.58	5.56 ± 0.48	5.48 ± 0.60	6.31 ± 0.68
40 gf	4.76 ± 0.36	5.54 ± 0.42	5.75 ± 0.57	5.68 ± 0.47	7.53 ± 0.33

Data are shown as means ± SD.

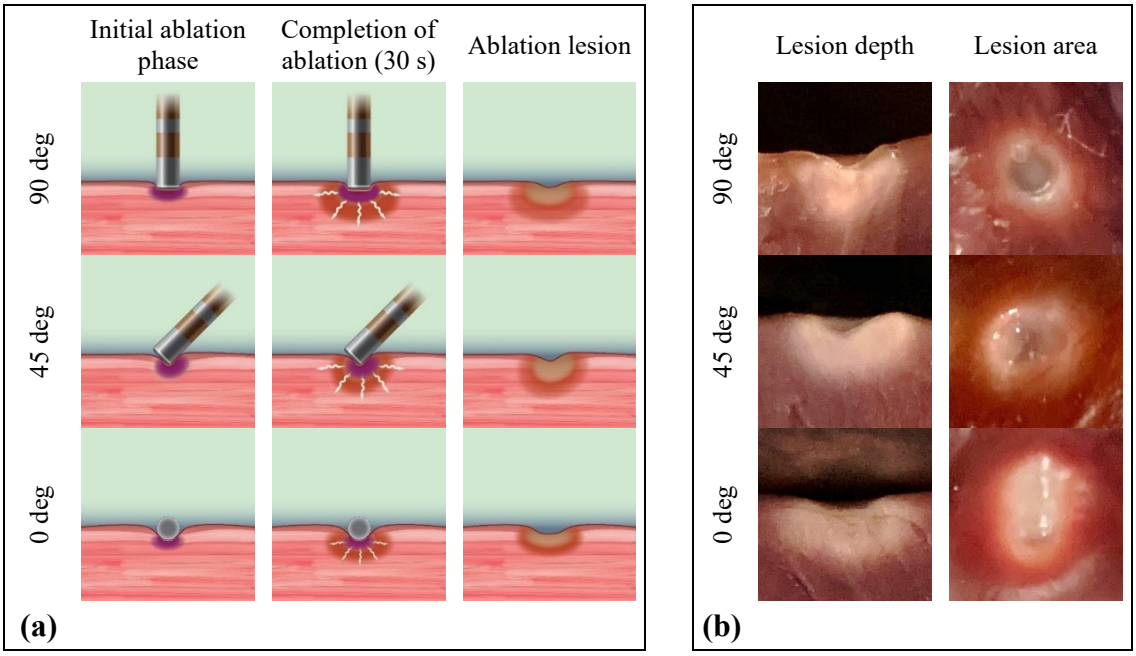

Figure 26. (a) Schematic illustration showing the differences in ablation lesion for each catheter contact angle. **(b)** Representative examples of lesion depth and lesion area for each contact angle at a contact force of 30 gf.

4.3.3 Relationships between ablation lesion area, catheter contact force, catheter contact angle, and catheter contact area

Figure 27 shows the positive correlations (r = 0.7816) between catheter contact force (x-axis) and lesion area (y-axis) at each contact angle. The results revealed that the lesion area increased significantly with increasing contact force ($P < 0.0001$ at every contact angle). Figure 28 is a plot of the correlation between catheter contact angle and lesion area for contact forces ranging from 2 to 40 gf. The results revealed that contact angle is a determinant of lesion area ($r = -0.3688$, $P = 0.0192$) (Table 10). The smallest lesion area was produced at a contact angle of 90 deg and increased with decreasing contact angle from 90 to 60, 45, 30, and 0 deg. There were no significant differences in lesion area at a contact angle of 0 vs. 30 deg, 30 vs. 45 deg, 45 vs. 60 deg, and 60 vs. 90 deg (95% confidence interval). However, significant differences were found in lesion area at a contact angle of 0 vs. 45, 60, and 90 deg; 30 vs. 60 and 90 deg; and 45 vs. 90 deg ($P < 0.05$) (Table 11). Figure 29 shows the positive correlation (r = 0.8507) between catheter contact area (x-axis) and lesion area (y-axis).

The results revealed that the lesion area increased significantly with increasing contact area ($P < 0.0001$).

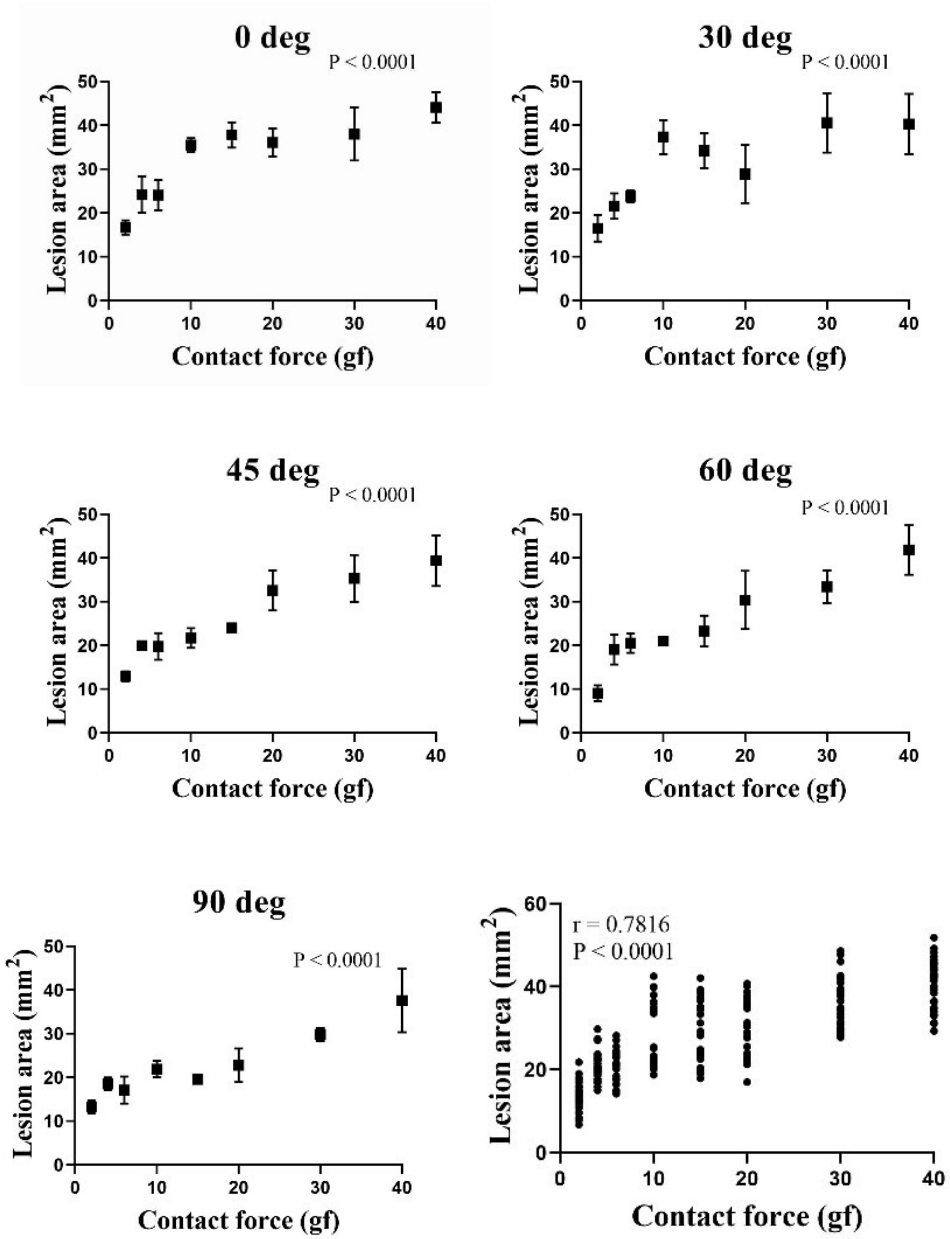

Figure 27. Correlation between catheter contact force and lesion area at each contact angle.

Table 10. Correlation between contact angle and lesion area and depth.

	Contact angle vs. lesion area	Contact angle vs. lesion depth
Pearson's r	−0.3688	0.4550
95% confidence interval	−0.6102 to −0.06470	0.1672 to 0.6714
P (two-tailed)	0.0192	0.0032
Significant? (alpha = 0.05)	Yes	Yes

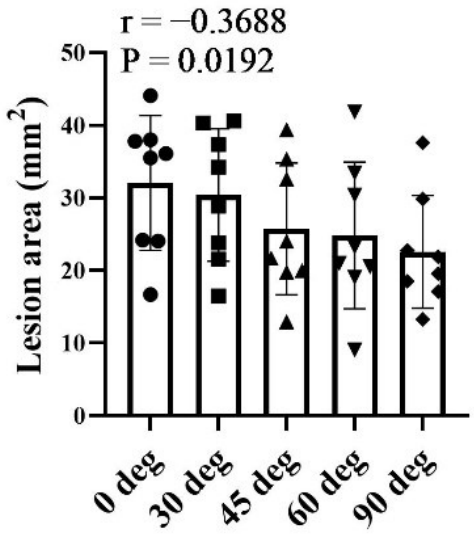

Figure 28. Lesion area as a function of contact force and contact angle.

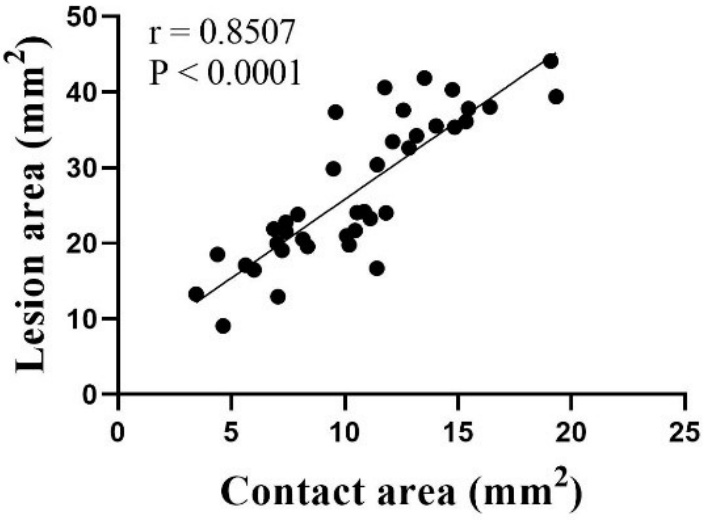

Figure 29. Correlation between the catheter contact area and lesion area.

Table 11. Comparison of lesion area and lesion depth at each contact angle.

Contact angle (deg)			Lesion area		Lesion depth	
			P-value	Significantly different (P < 0.05)?	P-value	Significantly different (P < 0.05)?
0	vs.	30	0.1928	No	0.8186	No
	vs.	45	0.0062	Yes	0.4129	No
	vs.	60	0.0036	Yes	0.0025	Yes
	vs.	90	0.0011	Yes	<0.0001	Yes
30	vs.	45	0.0605	No	0.3735	No
	vs.	60	0.0378	Yes	0.0063	Yes
	vs.	90	0.0037	Yes	<0.0001	Yes
45	vs.	60	0.2331	No	0.0291	Yes
	vs.	90	0.0342	Yes	<0.0001	Yes
60	vs.	90	0.1244	No	<0.0001	Yes

Table 12. Ratios of lesion area to contact area at each contact angle.

Contact angle	Contact force (gf)							
	2	4	6	10	15	20	30	40
0 deg	1.46	2.23	2.28	2.53	2.45	2.35	2.32	2.31
30 deg	2.74	2.91	3.00	3.89	2.60	1.97	3.45	2.73
45 deg	1.83	2.84	1.94	2.07	2.03	2.54	2.38	2.04
60 deg	1.95	2.63	2.51	2.08	2.09	2.66	2.76	3.10
90 deg	3.86	4.22	3.04	3.18	2.34	3.08	3.14	2.99

Table 12 shows the ratio of lesion area to contact area as a function of contact force and contact angle. The ratio of the ablation lesion area to the catheter contact area was calculated using the following equation; “Ratio of lesion area to contact area = (Ablated lesion area) / (Catheter contact area)”. The results revealed that catheter contact force had no significant relationship with the ratio of lesion area to contact area ($P = 0.5118$) and was only weakly correlated ($r_s = 0.1068$). Contact angle had a significant relationship with the ratio of lesion area to contact area ($P = 0.0175$) and was weakly correlated ($r_s = 0.3737$) (Table 13 and Figures. 30, 31, and 32).

Table 13. Correlation of contact force and contact angle with the ratio of lesion area to catheter contact area.

	Contact force vs. lesion area/contact area	Contact angle vs. lesion area/contact area
Spearman r_s	0.1068	0.3737
95% confidence interval	−0.2208 to 0.4128	0.06086 to 0.6196
P (two-tailed)	0.5118	0.0175
Significant? (alpha = 0.05)	No	Yes

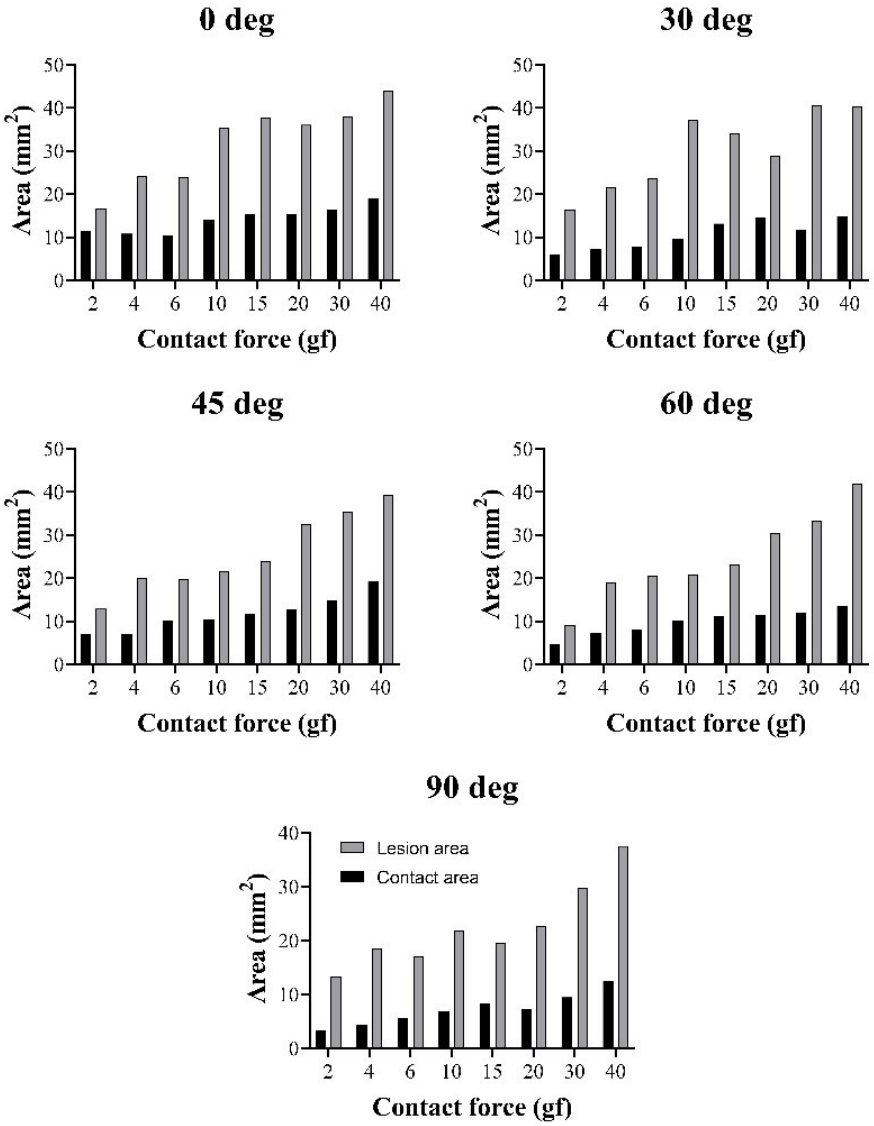

Figure 30. Comparison of the ratio of lesion area to catheter contact area at each contact angle.

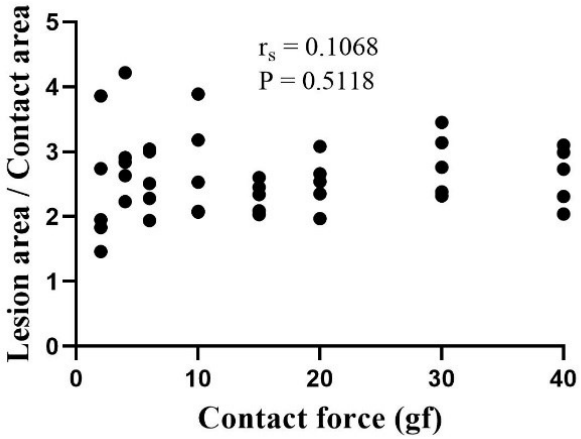

Figure 31. Correlation between catheter contact force and the ratio of lesion area to catheter contact area.

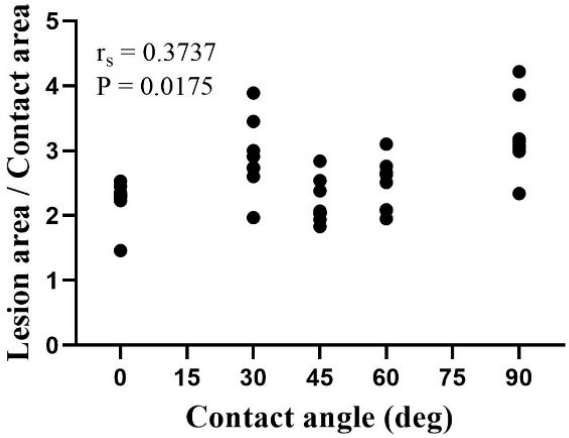

Figure 32. Correlation between catheter contact angle and the ratio of lesion area to catheter contact area.

4.3.4 Relationships between catheter contact force, catheter contact angle, and ablation lesion depth

Figure 33 shows the positive correlations (r = 0.7807) between catheter contact force (x-axis) and lesion depth (y-axis) at each contact angle. The results revealed that lesion depth increased significantly with increasing contact force ($P < 0.0001$ at every contact angle). Figure 34 is a plot of the correlation between catheter contact angle and lesion area for contact forces ranging from 2 to 40 gf. The results revealed that contact angle is a determinant of lesion depth ($r = 0.4550$, $P = 0.0032$) (Table 10). The smallest lesion depth was produced at a contact angle of 0 deg and increased with increasing contact angles from 0 to 30, 45, 60, and 90 deg. There were no significant differences

in lesion depth at a contact angle of 0 vs. 30 deg, 0 vs. 45, and 30 vs. 45 (95% confidence interval). However, significant differences were found in lesion depth at a contact angle of 0 vs. 60 and 90 deg; 30 vs. 60 and 90 deg; 45 vs. 60 and 90 deg; and 60 vs. 90 deg ($P < 0.05$) (Table 11). Further details will be discussed below in the Discussion section.

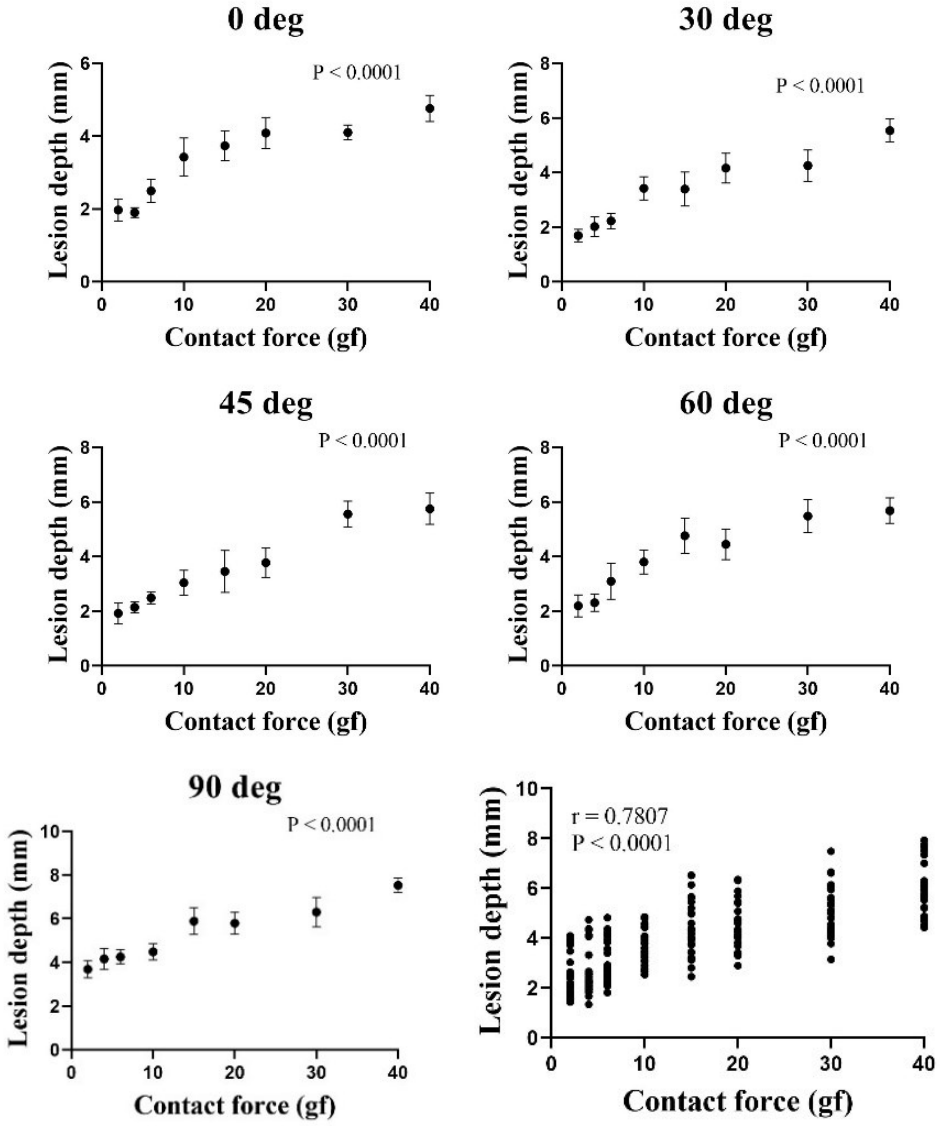

Figure 33. Correlation between catheter contact force and lesion depth at each contact angle.

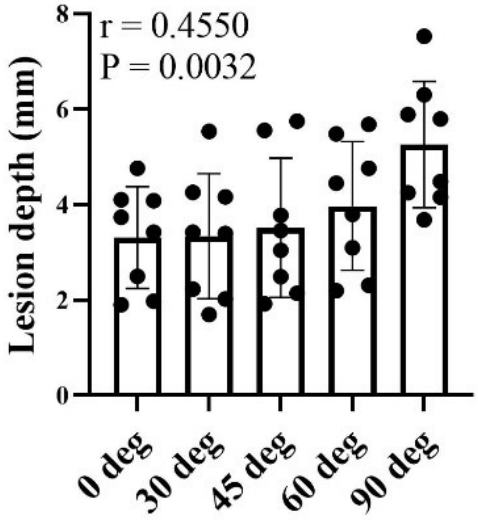

Figure 34. Lesion depth as a function of contact force and contact angle.

4.4 DISCUSSIONS

4.4.1 Correlation between catheter contact force and ablation impedance

The results of present study clearly demonstrated a significant positive correlation between the catheter contact force and the ablation impedance ($P < 0.0001$ at every contact angle). When the contact force was increased, the difference impedance between maximum impedance and average impedance also increased from Ohm's law relationship. Once impedance decreases, that means electrical current increases. Therefore, increased catheter contact force was associated with a corresponding increase in electrical current delivered to the heart tissue and also might be reduced electrical current flow into the blood, which is a cause of coagulum generation and failure to achieve appropriate myocardial temperatures [43]. However, the results showed only a different impedance between maximum impedance and average impedance due to this experimental systems' limitation. The impedance decreases were most often calculated by maximum impedance minus minimum impedance. Nevertheless, the experiment results as a whole showed a similar tendency with other previous studies [67, 68].

4.4.2 Correlation between percentage of contact area and ablation impedance

The previous study (Chapter 3) reported that increased contact force directly affects the percentage contact area of the tip electrode of an ablation catheter with the heart tissue surface (catheter contact area divided by catheter tip surface area). We hypothesized that the percentage of contact area might be correlated with ablation impedance. To test this hypothesis, the percentage of contact area was plotted on the x-axis and maximum impedance minus average impedance on the y-axis, as shown in Figure 35. The results revealed a significant positive correlation between the percentage of contact and the ablation impedance ($P < 0.0001$) When the percentage of contact area was increased, the difference impedance between maximum impedance and average impedance also increased.

4.4.3 No correlation between catheter contact angle and ablation impedance

Figure 36 shows the comparison between catheter contact force and maximum impedance minus average impedance at each contact angle. The ablation impedance at each contact angle did not significantly differ at a confidence level at 95% ($P < 0.05$). The possible reason for explaining this is the tip electrode's size, and the larger electrode will always deliver energy to heart tissue smaller than with a small electrode. In contrast, small tip electrodes will always deliver energy to heart tissue, even in a perpendicular or parallel orientation [45, 69]. Nakagawa H et al. [70] also reported that the power delivery from the 4 mm electrode to the heart tissue in perpendicular and parallel orientation was the same. Therefore, the results revealed interesting relationships among the parameters and the effect of catheter contact force and contact angle on the ablation impedance. To clearly confirm this point, the findings might be validated and explored in the near future experiments by developing an experimental system based on this present concept to measure the impedance decrease during ablation.

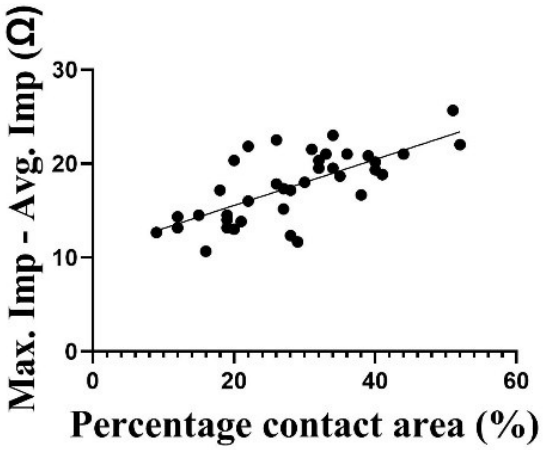

Figure 35. Correlation between percentage of contact area and the mean impedance between maximum impedance minus average impedance.

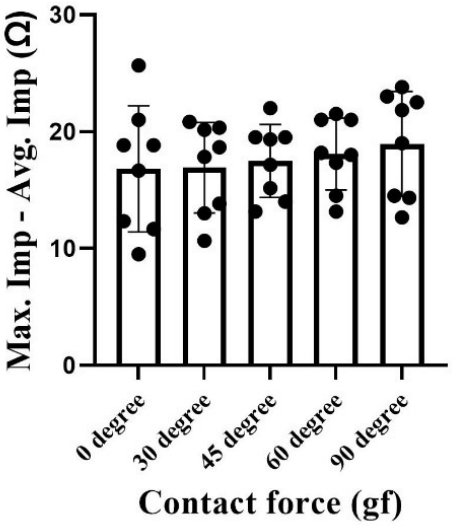

Figure 36. Comparison between catheter contact force and the mean impedance between maximum impedance minus average impedance at each contact angle.

4.4.4 Correlation between catheter contact area and ablation lesion area

The catheter–tissue contact area is a direct interface between the tip electrode of the ablation catheter and the surface of the heart tissue and depends on the contact conditions resulting from the combination of the contact force and contact angle. The electrical current delivered from the tip electrode of the ablation catheter passes through the contact area of the heart tissue surface and generates heat that raises the temperature of the tissue, causing the cells in that area to necrotize. Accordingly, the catheter contact area is an important consideration when planning ablation procedures.

Unfortunately, the attention this parameter receives does not match its importance. A possible reason for this may be the difficulty of visualizing the catheter–tissue contact area, which we successfully achieved in the previous study (Chapter 3). We speculated that the catheter contact area as a function of catheter contact force and catheter contact angle might substantially impact the size of the ablation lesion. We additionally hypothesized that the catheter contact area and lesion area morphology might be similar.

The results of the present study confirmed the hypotheses by revealing a very strong correlation between the catheter contact area and the ablation lesion area, as shown in Table 14. When the contact area was increased, the lesion area also increased. The relationship between catheter contact area and lesion area as a function of catheter contact angle and force can be summarized and expressed as the simple linear regression approximation formulas shown in Table 15. We also found that the lesion area morphology was almost the same as the catheter contact area. The lesion area morphology can be divided into three shapes: oval, circle, and ellipse, as shown in Figure 24b. In addition, we calculated the ratio of lesion area to contact area as a function of contact force and contact angle, as shown in Table 12. The results showed that catheter contact force had no significant relationship with the ratio of lesion area to contact area, whereas the contact angle did. Both also showed a very weak correlation with the ratio of lesion area to contact area. The contact area at a contact angle of 90 deg had the largest ratio compared with the same contact force at other contact angles. These data might describe the possible contact area at each angle and its relationship to the resulting lesion area. However, it should be noted that this amount of information may not be sufficient to conclude the exact contact area given that other factors were not considered.

Table 14. Correlation level and direction trend between each factor.

	Pearson's coefficient (r)*	Correlation level**
Contact force vs. lesion area	(+) 0.7816	Strong
Contact angle vs. lesion area	(−) 0.3688	Weak
Contact area vs. lesion area	(+) 0.8507	Very strong
Contact force vs. lesion depth	(+) 0.7807	Strong
Contact angle vs. lesion depth	(+) 0.4550	Moderate

*Positive values (+) denote positive correlations and negative values (−) denote negative correlations.

**Correlation level based on the absolute value of r: 0.00–0.19 is very weak, 0.20–0.39 is weak, 0.40–0.59 is moderate, 0.60–0.79 is strong, 0.80–1.0 is very strong, and a value of 0 denotes no correlation.

Table 15. Approximation formulas expressing the relationship between catheter contact area and ablation area as a function of contact force for each catheter contact angle.

Angle (deg)	Lesion area approximation formula	R^2	Contact area approximation formula	R^2
0	Y = 2.413X – 0.8227	0.9653	X = 2.685ln(Z) + 7.782	0.837
30	Y = 2.723X + 1.791	0.8799	X = 3.036ln(Z) + 3.465	0.845
45	Y = 2.079X + 1.395	0.8717	X = 3.689ln(Z) + 2.952	0.867
60	Y = 3.232X – 6.825	0.8709	X = 2.807ln(Z) + 3.137	0.984
90	Y = 2.601X + 4.486	0.9691	X = 2.693ln(Z) + 0.892	0.893

X is the catheter contact area (mm^2), Y is the ablation lesion area (mm^2), Z is the catheter contact force (gf), and R2 is the coefficient of determination (for $2 \leq Z \leq 40$).

4.4.5 Correlation between catheter contact force, ablation lesion area, and lesion depth

The catheter contact force showed a strongly positive correlation with ablation lesion area and depth, as shown in Table 14. When the contact force was increased, the lesion area and depth also increased. However, it is essential to consider the small changes in lesion area and depth that occurred at higher contact forces. As shown in Figs. 27 and 33, the slope of the graph changes slightly when the contact force is

between 15 and 40 gf and increases more during initial contact, when the contact force ranges from 2 to 15 gf. To clarify the behavior of the correlations among ablation lesion area, lesion depth, and catheter contact force, goodness of fit was calculated to facilitate comparison (Table 16 and Figure 37). The coefficient of determination (R^2) of each condition revealed that the lesion area increased monotonically but logarithmically at contact angles of 0, 30, 45, and 60 deg but not 90 deg. The lesion depth also increased logarithmically at contact angles of 0, 30, and 60 deg but not 45 and 90 deg. However, it should be noted that there was a slight difference in the value of R^2 under each condition.

The results of this study are not surprising; prior studies of ex vivo experimental models have also found a similar tendency for increasing catheter contact force to correlate with increasing lesion area and depth. Yokoyama et al. [39] performed irrigated-tip ablation at contact forces of 2, 10, 20, 30, and 40 gf using a canine thigh model. They found that increasing contact force was significantly associated with larger lesions. They concluded that the effect of catheter contact force was a more important determinant of lesion size compared with the delivered power. Thiagalingam et al. [63] also confirmed the importance of catheter contact force during irrigated ablation by using 3 different contact forces (2, 20, and 60 gf). They also concluded that catheter contact force has an important impact on ablation lesion size. Some evidence from in vivo studies and human studies have also shown the same tendency [54, 56, 58, 60].

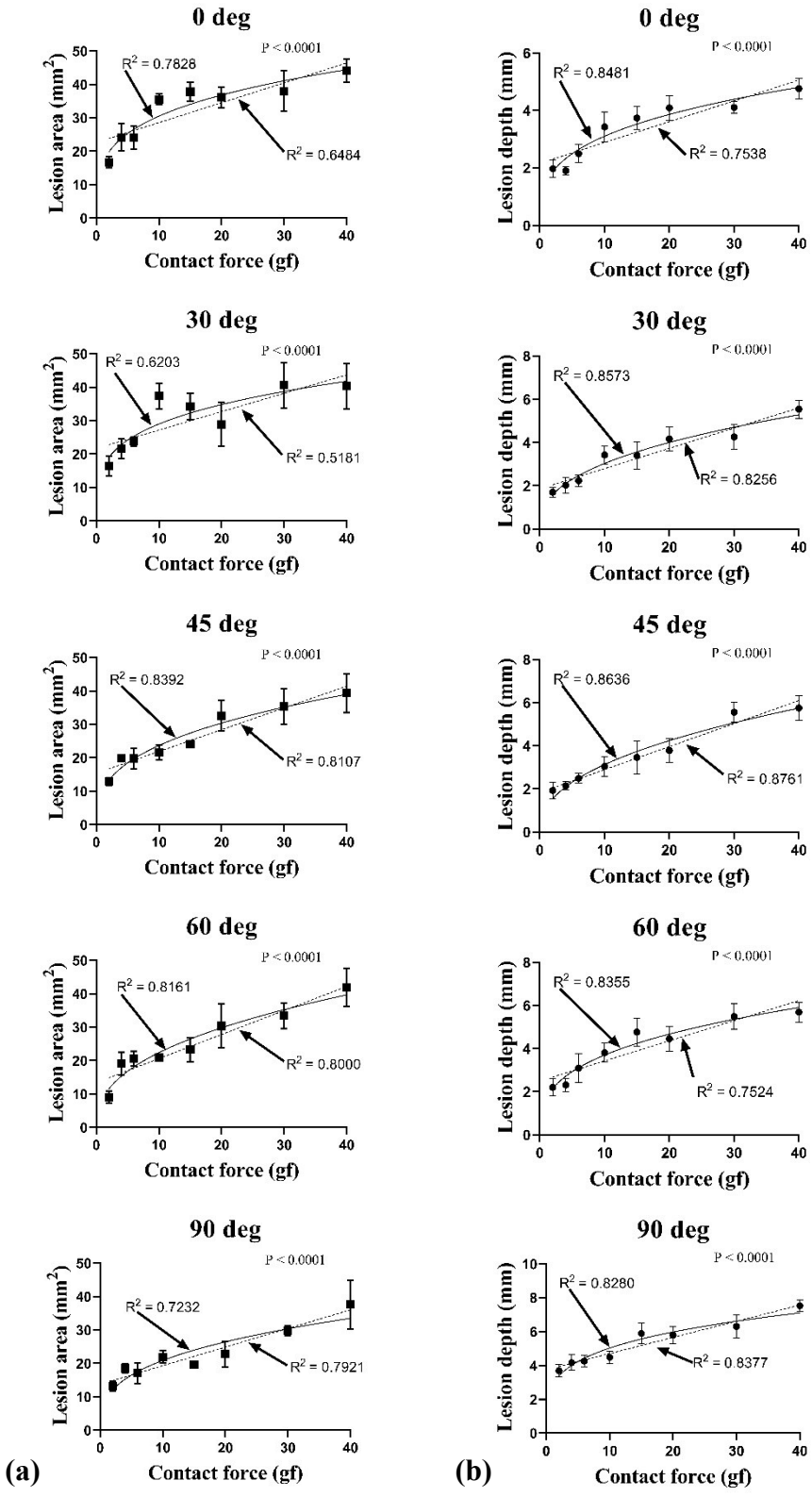

Figure 37. (a) Comparison (R^2) of the logarithmic and linear fit of the catheter contact angle with the lesion area; **(b)** Comparison (R^2) of the logarithmic and linear fit of the catheter contact angle with the lesion depth.

Table 16. Comparison (R^2) between the logarithmic and linear fit of the catheter contact force with lesion area and lesion depth at each contact angle.

Contact angle (deg)	Contact force vs. lesion area			Contact force vs. lesion depth		
	Logarithmic (R^2)	Linear (R^2)	Behavior of the correlation	Logarithmic (R^2)	Linear (R^2)	Behavior of the correlation
0	0.7828	0.6484	Log.	0.8481	0.7538	Log.
30	0.6203	0.5181	Log.	0.8573	0.8256	Log.
45	0.8392	0.8107	Log.	0.8636	0.8761	Linear
60	0.8161	0.8000	Log.	0.8355	0.7524	Log.
90	0.7232	0.7921	Linear	0.8280	0.8377	Linear

4.4.6 Correlation between catheter contact angle, ablation lesion area, and lesion depth

Catheter contact angle is a determinant of lesion area and depth, as shown in Table 14. However, the catheter contact angle and ablation lesion area are only weakly correlated. The lesion area progressively increased when the contact angle was decreased, as shown in Figure 28. The smallest lesion area was produced at a contact angle of 90 deg and increased with decreasing contact angle from 90 to 60, 45, 30, and 0 deg. The catheter contact angle and ablation lesion depth were moderately correlated. The lesion depth progressively increased when the contact angle was increased, as shown in Figure 34. The smallest lesion depth was produced at a contact angle of 0 deg and increased with increasing contact angle from 0 to 30, 45, 60, and 90 deg.

The catheter contact angle plays another role in lesion area morphology, as shown in Figure 26b. The lesion area morphology is oval (egg-like) when contact is made at an oblique catheter orientation (30, 45, and 60 deg). However, when contact is made at a parallel catheter orientation (0 deg), the lesion area morphology is an elliptical, whereas a perpendicular catheter orientation (90 deg) created a circular lesion area. Kawaji et al. [65] reported very similar results. They evaluated the lesion size in porcine hearts with an 8Fr open-tip irrigated catheter at 3 different contact angles (0, 45, and 90 deg), 3 levels of power (25, 30, and 35 W), and 3 contact forces (5, 15, and 30 gf). In their report, oblique and parallel catheter orientations created an

oval lesion area, whereas the perpendicular catheter orientation created a circular lesion area. In addition, they also concluded that the lesion depth significantly increased with a perpendicular rather than parallel orientation, but the lesion volume did not show a significant difference. Iwakawa et al. [64] also reported a similar tendency. They reported that a parallel catheter orientation created a significantly larger lesion area and a comparatively shallower lesion depth. Chan et al. [71] confirmed that the catheter orientation had a more pronounced effect on lesion dimensions compared with tip size alone. Lesions became larger with each increment in catheter tip length when the tip electrode was positioned parallel to the tissue surface. Calzolari et al. [72] also demonstrated that catheter contact angle plays a significant role in lesion size, but drew different conclusions. They used in vitro experimental model to create ablation lesions on a porcine heart with a fixed contact force of 20 gf at contact angles of 0, 45, and 90 deg. They concluded that the superficial lesion length increased as the catheter shifted from a perpendicular to a parallel orientation. The absolute maximal lesion length was greater with an oblique catheter orientation. However, their results showed that the lesion width was similar regardless of the orientation. This discrepancy between their findings and ours might be due to different experimental settings. In their study, the contact force was fixed at 20 gf, but we used various catheter contact forces ranging from 2 to 40 gf. In addition, differences in the catheter platform, including the shape of the catheter tip and irrigation rate, might also be a factor. Therefore, the effects of catheter contact angle on lesion dimensions require further investigation in order to provide sufficient knowledge that can be applied in the clinical setting.

4.5 MAJOR FINDINGS

The major findings are as follows. **(i),** catheter contact force has a significant correlation with ablation impedance. **(ii),** the ablation impedance did not significantly differ with each catheter contact angle. **(iii),** the catheter contact area showed a strong correlation with the ablation lesion area. When the contact area was increased, the

lesion area also increased linearly in a monotonic manner. **(IV),** the relationships between catheter contact force and ablation lesion area and between catheter contact force and ablation lesion depth are logarithmic functions in which increased contact force was associated with increased lesion area and depth. **(V),** the catheter contact angle is also an important determinant of the lesion area. The lesion area progressively increased when the contact angle was decreased. In contrast, the lesion depth progressively increased when the contact angle was increased.

4.6 CLINICAL IMPLICATIONS

Precise control of lesion dimensions is an essential parameter for treatment strategies. Catheter contact area might be another effective parameter for controlling the ablation lesion dimensions, given that the catheter contact area is a direct interface between the tip electrode of the ablation catheter and the surface of the heart tissue. However, the data obtained in this study cannot be applied directly to clinical practice on a beating human heart, especially in terms of lesion size. Nevertheless, the findings of the present study support a possible role of catheter contact area imaging for assessing ablation lesion dimension. This study provides data showing a very strong correlation between catheter contact area and ablation lesion area. It also provides approximation formulas for estimating lesion area as a function of contact area and contact force for each contact angle. These data should help clinicians performing this procedure to understand the relationships among the parameters and plan their experiment strategy accordingly. Lastly, these data suggest that the extent to which lesion size can be increased by increasing the contact force may be limited. The catheter contact angle relative to the surface of the heart muscle tissue should also be considered when calculating the desired lesion size.

4.7 STUDY LIMITATIONS

This study has several limitations. First, this study was conducted using an ex vivo model consisting of a porcine heart, so there was no respiratory motion, catheter instability, or cardiac beating. However, because a precisely controlled model was

required to achieve the purpose of this study, the ex vivo model was deemed appropriate for this study. In addition, the experimental heart model did not include coronary perfusion and used saline instead of blood (saline has a higher electrical conductivity compared with blood). Therefore, the results cannot be applied directly to clinical practice on a beating human heart, especially in terms of lesion size. Second, the instrument used in this study features a heart muscle surface flattener and a catheter-tip-angle setter in order to ensure reproducibility. However, in clinical practice, the shape of the heart tissue surface varies according to the part of the heart, and thus the catheter tip orientation can rarely be optimized due to the various anatomical structures of the heart. Nevertheless, to achieve the purpose of this study, it was necessary to perform tests on flat surfaces to clearly show the effects of the investigated parameters on the surface of the heart tissue. Third, this study used an open-loop irrigated catheter tip, specifically a "flat-tip catheter," with a pre-determined size and width. Thus, these results might not be reproducible with other commercially available catheters. Lastly, the approximation formulas for estimating contact and lesion area are limited to procedures using the same ablation parameters as in this study. However, the results revealed interesting relationships among the parameters as well as the effect of catheter contact force and contact angle on the contact area and lesion dimensions. Thus, the findings should be further investigated by conducting in vivo experiments, animal model experiments, or studies based on practical clinical treatment.

4.8 CONCLUSION

The present study showed an important role of the catheter contact force on the ablation impedance in RF catheter ablation procedures, while contact angle did not. The results showed a significant positive correlation between the percentage of contact area and ablation impedance. Moreover, this study revealed a strongly significant positive correlation between catheter contact area and ablation lesion area. The findings clearly demonstrated a substantial impact of catheter contact force, contact

angle, and contact area on lesion dimensions in RF catheter ablation procedures. Such information should be helpful in the selection of effective values for contact force and contact angle in order to predict lesion size as well as for clinicians performing this procedure to understand the relationships among the parameters and plan their ablation strategy accordingly.

Chapter 5: Future Work

During this research study, we had several discussions with advisors and researchers, then we got sparked ideas of further application and development of the effects of the catheter contact force and contact angle on contact area and lesion dimension. Proposed further works are described in detail in the following sections.

5.1 FURTHER APPLICATION

5.1.1 Ablation lesion prediction

This study is an ex vivo model consisting of a porcine heart. Therefore, the results cannot be applied directly to clinical practice on a beating human heart, especially in terms of lesion size. However, the results based on this study, especially the lesion area approximation formulas, might be developed further by validating data through numerical simulations such as the Finite Elemental Method or a practical investigation through an in vivo heart muscle ablation experiment. Later, the approximation formulas expressing the relationship between catheter contact area and ablation area as a function of contact force for each catheter contact angle as presented in this research might be helpful for estimating contact and lesion area in clinical practice in the near future.

5.1.2 The application of this experimental system to measure complex impedance

Another interesting application of the presented study is an application of this experimental system to investigate ablation impedance in detail. Measuring the complex impedance relative to contact force and angle during an entire ablation duration is challenging work. The main focused parameter of this study is the contact condition that comprises contact force and angle. Those parameters correspond to the ablation impedance (resistance) that is divided into two components. The first is the resistance between the catheter tip and the heart tissue surface. The second is the resistance between the catheter tip and blood. Therefore, future work with applying

this experimental system could potentially unlock the ability to support a possible role of catheter contact condition for assessing ablation lesion dimension.

5.2 FURTHER RESEARCH

5.2.1 Lesion formation on epicardial adipose tissue

In this study, only the surface of a portion of epicardium lacking adipose tissue was ablated. During the experiment, we founded that an ablated on the heart tissue with adipose was ineffective to create ablation lesion and poor lesion formation. For this reason, in this study, we avoided to ablate the adipose area on the heart tissue. However, ventricular tachycardia (VT) origin sometimes found in the epicardial. In some cases, the anatomic area of epicedial adipose sometimes corresponded with desired targets for ablation, which unable to avoid.

Nowadays, there are very few pieces of evidence on these issues. Against this backdrop, the lesion formation of the heart muscle with adipose tissue as a function of catheter contact force and angle very interesting to investigate.

5.2.2 Catheter stability

This present study successfully developed the experimental system that enables set the precision catheter contact angle with respect to the heart muscle's surface and the catheter contact force. This system ensures the stability of the catheter contact without tip slide during ablation across various forces and angles. We hypothesized that maintaining contact condition stability might significantly affect the efficient transfer of RF energy into the tissue. Therefore, the efficiency of catheter stability under controllable contact force and angle might be interesting to apply this experimental system to investigate.

Chapter 6: Conclusion

The results of this study clearly demonstrated a substantial impact of the contact angle and contact force of a catheter on the size and morphology of the contact area in catheter ablation procedures. Moreover, the present study showed an important role of the catheter contact force on the ablation impedance in RF catheter ablation procedures, while contact angle did not. The findings showed a significant positive correlation between the percentage of contact area and ablation impedance. In addition, this study revealed a strongly significant positive correlation between catheter contact area and ablation lesion area. The findings clearly demonstrated a substantial impact of catheter contact force, contact angle, and contact area on lesion dimensions in RF catheter ablation procedures.

The work presented in this thesis was predominantly a theoretical modelling study conducted using an ex vivo model consisting of a porcine heart, so there was no respiratory motion, catheter instability, or cardiac beating. Therefore, the results cannot be applied directly to clinical practice on a beating human heart, especially in terms of lesion size. Nevertheless, the findings of this study support a possible role of catheter contact area imaging for assessing ablation lesion dimensions. This study provides data showing a very strong correlation between catheter contact area and ablation lesion area. It also provides approximation formulas for estimating lesion area as a function of contact area and contact force for each contact angle. These data should help clinicians performing this procedure to understand the relationships among the parameters and plan their ablation strategy accordingly. Lastly, these data suggest that the extent to which lesion size can be increased by increasing the contact force may be limited. The catheter contact angle relative to the surface of the heart muscle tissue should also be considered when calculating the desired lesion size.

In contemporary clinical practice, precise control of lesion dimensions is an essential parameter for treatment strategies. The catheter contact area might be another

effective parameter for controlling the ablation lesion dimensions, given that the catheter contact area is a direct interface between the tip electrode of the ablation catheter and the surface of the heart tissue. Such information should be helpful in the selection of effective values for contact force and contact angle in order to predict lesion size as well as for clinicians performing this procedure to understand the relationships among the parameters and plan their ablation strategy accordingly.

Bibliography

1. WHO (2017) Cardiovascular Diseases. In: world Heal. Organ. https://www.who.int/en/news-room/fact-sheets/detail/cardiovascular-diseases-(cvds)

2. Colilla S, Crow A, Petkun W, Singer DE, Simon T, Liu X (2013) Estimates of current and future incidence and prevalence of atrial fibrillation in the U.S. adult population. Am J Cardiol 112:1142–1147 . https://doi.org/10.1016/j.amjcard.2013.05.063

3. Rodney J Levick (2010) An Introduction to Cardiovascular Physiology, 5th ed. Hodder Education Publishers, London, UK

4. Zheng J, Zhang J, Danioko S, Yao H, Guo H, Rakovski C (2020) A 12-lead electrocardiogram database for arrhythmia research covering more than 10,000 patients. Sci Data 7:1–8 . https://doi.org/10.1038/s41597-020-0386-x

5. Hu R, Stevenson WG, Strichartz GR, Lilly LS (2013) Mechanisms of cardiac arrhythmias. Pathophysiol Hear Dis A Collab Proj Med Students Fac Fifth Ed 65:261–278 . https://doi.org/10.1016/j.rec.2011.09.020

6. Antzelevitch C, Burashnikov A (2011) Overview of Basic Mechanisms of Cardiac Arrhythmia. Card Electrophysiol Clin 3:23–45 . https://doi.org/10.1016/j.ccep.2010.10.012

7. Coumel P. (1989) Classification of Human Arrhythmias. In: E.M. VW (ed) Antiarrhythmic Drugs. Handbook of Experimental Pharmacology, vol 89. Springer, Berlin, Heidelberg, pp 87–103

8. Ponikowski P, Voors AA, Anker SD, Bueno H, Cleland JGF, Coats AJS, Falk V, González-Juanatey JR, Harjola VP, Jankowska EA, Jessup M, Linde C, Nihoyannopoulos P, Parissis JT, Pieske B, Riley JP, Rosano GMC, Ruilope LM, Ruschitzka F, Rutten FH, Van Der Meer P, Sisakian HS, Isayev E, Kurlianskaya A, Mullens W, Tokmakova M, Agathangelou P, Melenovsky V, Wiggers H, Hassanein M, Uuetoa T, Lommi J, Kostovska ES, Juilliere Y, Aladashvili A, Luchner A, Chrysohoou C, Nyolczas N, Thorgeirsson G, Weinstein JM, Lenarda A Di, Aidargaliyeva N, Bajraktari G, Beishenkulov M, Kamzola G, Abdel-Massih T, Celutkiene J, Noppe S, Cassar A, Vataman E, AbirKhalil S, van Pol P, Mo R, Straburzynska-Migaj E, Fonseca C, Chioncel O, Shlyakhto E, Zavatta M, Otasevic P, Goncalvesova E, Lainscak M, Molina BD, Schaufelberger M, Suter T, Yılmaz MB, Voronkov L, Davies C (2016) 2016 ESC Guidelines for the diagnosis and treatment of acute and chronic heart failure. Eur Heart J 37:2129-2200m . https://doi.org/10.1093/eurheartj/ehw128

9. Shenthar J (2015) Unusual Incessant Ventricular Tachycardia: What Is the Underlying Cause and the Possible Mechanism? Circ Arrhythmia Electrophysiol 8:1507–1511 . https://doi.org/10.1161/CIRCEP.115.002886

10. Srinivasan NT, Schilling RJ (2018) Sudden cardiac death and arrhythmias. Arrhythmia Electrophysiol Rev 7:111–117 .

https://doi.org/10.15420/aer.2018.15.2

11. Kobayashi Y (2018) How to manage various arrhythmias and sudden cardiac death in the cardiovascular intensive care. J Intensive Care 6:1–15 . https://doi.org/10.1186/s40560-018-0292-x

12. Cooper AS (2020) Antiarrhythmics for maintaining sinus rhythm after cardioversion of atrial fibrillation. Crit Care Nurse 40:79–81 . https://doi.org/10.4037/ccn2020161

13. Marrouche NF, Brachmann J, Andresen D, Siebels J, Boersma L, Jordaens L, Merkely B, Pokushalov E, Sanders P, Proff J, Schunkert H, Christ H, Vogt J, Bänsch D (2018) Catheter Ablation for Atrial Fibrillation with Heart Failure. N Engl J Med 378:417–427 . https://doi.org/10.1056/nejmoa1707855

14. Borggrefe M, Budde T, Podczeck A, Breithardt G (1987) High frequency alternating current ablation of an accessory pathway in humans. J Am Coll Cardiol 10:576–582 . https://doi.org/10.1016/S0735-1097(87)80200-0

15. Odell RC, Lev M (1987) Closed chest catheter desiccation of the atrioventricular junction using radiofrequency energy—A new method of catheter ablation. J Am Coll Cardiol 9:349–358 . https://doi.org/10.1016/S0735-1097(87)80388-1

16. Yonas E, Pranata R, Siswanto BB, Abdulgani HB (2020) Comparison between surgical and catheter based ablation in atrial fibrillation, should surgical based ablation be implemented as first line? - A meta-analysis of studies. Indian Pacing Electrophysiol J 20:14–20 . https://doi.org/10.1016/j.ipej.2019.12.001

17. Hosseini SM, Rozen G, Saleh A, Vaid J, Biton Y, Moazzami K, Heist EK, Mansour MC, Kaadan MI, Vangel M, Ruskin JN (2017) Catheter Ablation for Cardiac Arrhythmias: Utilization and In-Hospital Complications, 2000 to 2013. JACC Clin Electrophysiol 3:1240–1248 . https://doi.org/10.1016/j.jacep.2017.05.005

18. Grubb CS, Lewis M, Whang W, Biviano A, Hickey K, Rosenbaum M, Garan H (2019) Catheter Ablation for Atrial Tachycardia in Adults With Congenital Heart Disease: Electrophysiological Predictors of Acute Procedural Success and Post-Procedure Atrial Tachycardia Recurrence. JACC Clin Electrophysiol 5:438–447 . https://doi.org/10.1016/j.jacep.2018.10.011

19. Sohns C, Nürnberg JH, Hebe J, Duckeck W, Ventura R, Konietschke F, Cao C, Siebels J, Volkmer M (2018) Catheter Ablation for Atrial Fibrillation in Adults With Congenital Heart Disease: Lessons Learned From More Than 10 Years Following a Sequential Ablation Approach. JACC Clin Electrophysiol 4:733–743 . https://doi.org/10.1016/j.jacep.2018.01.015

20. Ichijo S, Miyazaki S, Kusa S, Nakamura H, Hachiya H, Kajiyama T, Iesaka Y (2018) Impact of catheter ablation of atrial fibrillation on long-term clinical outcomes in patients with heart failure. J Cardiol 72:240–246 . https://doi.org/10.1016/j.jjcc.2018.02.012

21. Page RL, Joglar JA, Caldwell MA, Calkins H, Conti JB, Deal BJ, Estes NAM, Field ME, Goldberger ZD, Hammill SC, Indik JH, Lindsay BD, Olshansky B,

Russo AM, Shen WK, Tracy CM, Al-Khatib SM (2016) 2015 ACC/AHA/HRS guideline for the management of adult patients with supraventricular tachycardia: A report of the American College of Cardiology/American Heart Association Task Force on Clinical Practice Guidelines and the Heart Rhythm Society

22. Nath S, Lynch C, Whayne JG, Haines DE (1993) Cellular electrophysiological effects of hyperthermia on isolated guinea pig papillary muscle: Implications for catheter ablation. Circulation 88:1826–1831 . https://doi.org/10.1161/01.CIR.88.4.1826

23. Dewhirst MW, Viglianti BL, Lora-Michiels M, Hanson M, Hoopes PJ (2003) Basic principles of thermal dosimetry and thermal thresholds for tissue damage from hyperthermia. Int J Hyperth 19:267–294 . https://doi.org/10.1080/0265673031000119006

24. WITTKAMPF FHM, SIMMERS TA, HAUER RNW, ROBLES de MEDINA EO (1995) Myocardial Temperature Response During Radiofrequency Catheter Ablation. Pacing Clin Electrophysiol 18:307–317 . https://doi.org/10.1111/j.1540-8159.1995.tb02521.x

25. Haines DE, Verow AF (1990) Observations on electrode-tissue interface temperature and effect on electrical impedance during radiofrequency ablation of ventricular myocardium. Circulation 82:1034–1038 . https://doi.org/10.1161/01.CIR.82.3.1034

26. Langberg JJ (1993) Temperature monitoring during radiofrequency catheter ablation. Circulation 87:656 . https://doi.org/10.1161/circ.87.2.8489581

27. NATH S, DiMARCO JP, HAINES DE (1994) Basic Aspects of Radiofrequency Catheter Ablation. J Cardiovasc Electrophysiol 5:863–876 . https://doi.org/10.1111/j.1540-8167.1994.tb01125.x

28. Haines DE, Watson DP, Verow AF (1990) Electrode radius predicts lesion radius during radiofrequency energy heating. Validation of a proposed thermodynamic model. Circ Res 67:124–129 . https://doi.org/10.1161/01.RES.67.1.124

29. Jones JL, Lepeschkin E, Jones RE RS (1978) Response of cultured myocardial cells to countershock-type electric field stimulation. Am J Physiol Aug;235(2):14–22 . https://doi.org/10.1152/ajpheart.1978.235.2.H214

30. Editors: Schmitt, C., Deisenhofer, I., Zrenner B (2006) Catheter Ablation of Cardiac Arrhythmias: A Practical Approach, 1st ed. Steinkopff, Deutsches Herzzentrum MünchenMünchenGermany

31. Jones JL, Proskauer CC, Paull WK, Lepeschkin E, Jones RE (1980) Ultrastructural injury to chick myocardial cells in vitro following “electric countershock.” Circ Res 46:387–394 . https://doi.org/10.1161/01.RES.46.3.387

32. Müssigbrodt A, Grothoff M, Dinov B, Kosiuk J, Richter S, Sommer P, Breithardt OA, Rolf S, Bollmann A, Arya A, Hindricks G (2015) Irrigated Tip Catheters for Radiofrequency Ablation in Ventricular Tachycardia. BioMed Res Int 2015:

33. Siroky GP, Hazari M, Younan Z, Patel A, Balog J, Rudnick A, Kassotis J, Kostis WJ, Coromilas J, Saluja D (2020) Irrigated vs. Non-irrigated Catheters in the Ablation of Accessory Pathways. J Cardiovasc Transl Res 13:612–617 . https://doi.org/10.1007/s12265-019-09926-w

34. WEISS, C., ANTZ, M., EICK, O., ESHAGZAIY, K., MEINERTZ, T. and WILLEMS S (2002) Radiofrequency Catheter Ablation Using Cooled Electrodes: Impact of Irrigation Flow Rate and Catheter Contact Pressure on Lesion Dimensions. Pacing Clin Electrophysiol 25:463–469 . https://doi.org/10.1046/j.1460-9592.2002.00463.x

35. Yokoyama K, Nakagawa H, Wittkampf FHM, Pitha J V., Lazzara R, Jackman WM (2006) Comparison of electrode cooling between internal and open irrigation in radiofrequency ablation lesion depth and incidence of thrombus and steam pop. Circulation 113:11–19 . https://doi.org/10.1161/CIRCULATIONAHA.105.540062

36. Barnett AS, Bahnson TD, Piccini JP (2016) Recent Advances in Lesion Formation for Catheter Ablation of Atrial Fibrillation. Circ Arrhythmia Electrophysiol 9:1–9 . https://doi.org/10.1161/CIRCEP.115.003299

37. AVITALL, B., MUGHAL, K., HARE, J., HELMS, R. and KRUM D (1997) The Effects of Electrode-Tissue Contact on Radiofrequency Lesion Generation. Pacing Clin Electrophysiol 20:2899–2910 . https://doi.org/10.1111/j.1540-8159.1997.tb05458.x

38. OKUMURA, Y., JOHNSON, S.B., BUNCH, T.J., HENZ, B.D., O'BRIEN, C.J. and PACKER DL (2008) A Systematical Analysis of In Vivo Contact Forces on Virtual Catheter Tip/Tissue Surface Contact during Cardiac Mapping and Intervention. J Cardiovasc Electrophysiol 19:632–640 . https://doi.org/10.1111/j.1540-8167.2008.01135.x

39. Yokoyama K, Nakagawa H, Shah DC, Lambert H, Leo G, Aeby N, Ikeda A, Pitha J V., Sharma T, Lazzara R, Jackman WM (2008) Novel contact force sensor incorporated in irrigated radiofrequency ablation catheter predicts lesion size and incidence of steam pop and thrombus. Circ Arrhythm Electrophysiol 1:354–362 . https://doi.org/10.1161/CIRCEP.108.803650

40. Nakagawa H, Jackman WM (2014) The role of contact force in atrial fibrillation ablation. J Atr Fibrillation 7:78–84 . https://doi.org/10.4022/jafib.1027

41. SHAH, D.C., LAMBERT, H., NAKAGAWA, H., LANGENKAMP, A., AEBY, N. and LEO G (2010) Area Under the Real-Time Contact Force Curve (Force–Time Integral) Predicts Radiofrequency Lesion Size in an In Vitro Contractile Model. J Cardiovasc Electrophysiol 21:1038–1043 . https://doi.org/10.1111/j.1540-8167.2010.01750.x

42. Takami M, Lehmann HI, Parker KD, Welker KM, Johnson SB, Packer DL (2016) Effect of left atrial ablation process and strategy on microemboli formation during irrigated radiofrequency catheter ablation in an in vivo model. Circ Arrhythmia Electrophysiol 9: . https://doi.org/10.1161/CIRCEP.115.003226

43. J M Kalman, A P Fitzpatrick, J E Olgin, M C Chin, R J Lee, M M Scheinman

MDL (1997) Biophysical characteristics of radiofrequency lesion formation in vivo: dynamics of catheter tip-tissue contact evaluated by intracardiac echocardiography. Am Hear J 133:8–18 . https://doi.org/10.1016/s0002-8703(97)70242-4

44. Iso K, Okumura Y, Watanabe I, Nagashima K, Sonoda K, Kogawa R, Sasaki N, Takahashi K, Kurokawa S, Nakai T, Ohkubo K, Hirayama A (2016) Wall thickness of the pulmonary vein-left atrial junction rather than electrical information as the major determinant of dormant conduction after contact force-guided pulmonary vein isolation. J Interv Card Electrophysiol 46:325–333 . https://doi.org/10.1007/s10840-016-0147-0

45. Tsai CF, Tai CT, Yu WC, Chen YJ, Hsieh MH, Chiang CE, Ding YA, Chang MS, Chen SA (1999) Is 8-mm more effective than 4-mm tip electrode catheter for ablation of typical atrial flutter? Circulation 100:768–771 . https://doi.org/10.1161/01.CIR.100.7.768

46. David Haines (2004) Biophysics of Ablation: Application to Technology. J Cardiovasc Electrophysiol 15:S2–S11 . https://doi.org/10.1046/j.1540-8167.2004.15102.x

47. WITTKAMPF, F.H. and NAKAGAWA H (2006) RF Catheter Ablation: Lessons on Lesions. Pacing Clin Electrophysiol 29:1285–1297 . https://doi.org/10.1111/j.1540-8159.2006.00533.x

48. Iwasawa J, Koruth JS, Petru J, Dujka L, Kralovec S, Mzourkova K, Dukkipati SR, Neuzil P, Reddy VY (2017) Temperature-Controlled Radiofrequency Ablation for Pulmonary Vein Isolation in Patients With Atrial Fibrillation. J Am Coll Cardiol 70:542–553 . https://doi.org/10.1016/j.jacc.2017.06.008

49. Franco E, Rodríguez Muñoz D, Matía R, Hernández-Madrid A, Sánchez Pérez I, Zamorano JL, Moreno J (2018) Contact force-sensing catheters: performance in an ex vivo porcine heart model. J Interv Card Electrophysiol 53:141–150 . https://doi.org/10.1007/s10840-018-0435-y

50. Shah DC, Namdar M (2015) Real-Time Contact Force Measurement: A Key Parameter for Controlling Lesion Creation with Radiofrequency Energy. Circ Arrhythmia Electrophysiol 8:713–721 . https://doi.org/10.1161/CIRCEP.115.002779

51. Ariyarathna N, Kumar S, Thomas SP, Stevenson WG, Michaud GF (2018) Role of Contact Force Sensing in Catheter Ablation of Cardiac Arrhythmias: Evolution or History Repeating Itself? JACC Clin Electrophysiol 4:707–723 . https://doi.org/10.1016/j.jacep.2018.03.014

52. Fuller IA, Wood MA (2003) Intramural coronary vasculature prevents transmural radiofrequency lesion formation: Implications for linear ablation. Circulation 107:1797–1803 . https://doi.org/10.1161/01.CIR.0000058705.97823.F4

53. Simmers TA, De Bakker JMT, Coronel R, Wittkampf FHM, Van Capelle FJ, Janse MJ, Hauer RNW (1998) Effects of intracavitary blood flow and electrode-target distance on radiofrequency power required for transient conduction block in a Langendorff-perfused canine model. J Am Coll Cardiol 31:231–235 .

https://doi.org/10.1016/S0735-1097(97)00435-X

54. Sacher F, Wright M, Derval N, Denis A, Ramoul K, Pascale P, Bordachar P, Ritter P, Hocini M, Santos P Dos, Haissaguerre M, Jais P (2013) Endocardial Versus Epicardial Ventricular Radiofrequency Ablation Utility of In Vivo Contact Force Assessment. Circ Arrhythmia Electrophysiol 6:144–151 . https://doi.org/10.1161/CIRCEP.11

55. Ho SY, Cabrera JA, Tran VH, Farré J, Anderson RH, Brompton R, Trust HNHS (2001) Architecture of the pulmonary veins: relevance to radiofrequency ablation. Heart 1:265–270

56. Conti S, Weerasooriya R, Novak P, Champagne J, Lim HE, Macle L, Khaykin Y, Pantano A, Verma A (2018) Contact force sensing for ablation of persistent atrial fibrillation: A randomized, multicenter trial. Hear Rhythm 15:201–208 . https://doi.org/10.1016/j.hrthm.2017.10.010

57. Rune Borregaard, Henrik Kjærulf Jensen, Bawer Jalal Tofig, Samuel Alberg Thrysøe, Christian Gerdes JCN& PL (2017) Is the knowledge of contact force beneficial in pulmonary vein antrum isolation? Scand Cardiovasc J 51:129–137 . https://doi.org/10.1080/14017431.2017.1285043

58. Ullah W, McLean A, Tayebjee MH, Gupta D, Ginks MR, Haywood GA, O'Neill M, Lambiase PD, Earley MJ, Schilling RJ (2016) Randomized trial comparing pulmonary vein isolation using the SmartTouch catheter with or without real-time contact force data. Hear Rhythm 13:1761–1767 . https://doi.org/10.1016/j.hrthm.2016.05.011

59. Ikeda A, Nakagawa H, Lambert H, Shah DC, Fonck E, Yulzari A, Sharma T, Pitha J V., Lazzara R, Jackman WM (2014) Relationship between catheter contact force and radiofrequency lesion size and incidence of steam pop in the beating canine heart: Electrogram amplitude, impedance, and electrode temperature are poor predictors of electrode-tissue contact force and lesion. Circ Arrhythmia Electrophysiol 7:1174–1180 . https://doi.org/10.1161/CIRCEP.113.001094

60. Ullah W, Hunter RJ, Baker V, Dhinoja MB, Sporton S, Earley MJ, Schilling RJ (2014) Target indices for clinical ablation in atrial fibrillation: Insights from contact force, electrogram, and biophysical parameter analysis. Circ Arrhythmia Electrophysiol 7:63–68 . https://doi.org/10.1161/CIRCEP.113.001137

61. Nakagawa, H., Atsushi Ikeda, A. Govari, T. Papaioannou, G. Constantine, M. Bar-Tal, Erez Silberschein, Eitan Saba-Keren, Assaf Rubissa, Tushar Sharma, J. Pitha RL and WJ (2013) Abstract 12104: Prospective Study Using a New Formula Incorporating Contact Force, Radiofrequency Power and Application Time (Force-Power-Time Index) for Quantifying Lesion Formation to Guide Long Continuous Atrial lesions in the Beating Canine Heart. Circ J 128:

62. Münkler P, Kröger S, Liosis S, Abdin A, Lyan E, Eitel C, Eitel I, Meyer C, Willems S, Heeger CH, Tilz RR (2018) Ablation index for catheter ablation of atrial fibrillation: Clinical applicability and comparison with force-time integral. Circ J 82:2722–2727 . https://doi.org/10.1253/circj.CJ-18-0361

63. Thiagalingam A, D'Avila A, Foley L, Guerrero JL, Lambert H, Leo G, Ruskin JN, Reddy VY (2010) Importance of catheter contact force during irrigated radiofrequency ablation: Evaluation in a porcine ex vivo model using a force-sensing catheter. J Cardiovasc Electrophysiol 21:806–811 . https://doi.org/10.1111/j.1540-8167.2009.01693.x

64. Iwakawa H, Takigawa M, Goya M, Iwata T, Martin CA, Anzai T, Takahashi K, Amemiya M, Yamamoto T, Sekigawa M, Shirai Y, Tao S, Hayashi T, Takahashi Y, Watanabe H, Sasano T (2021) Clinical implications of local impedance measurement using the IntellaNav MiFi OI ablation catheter: an ex vivo study. J Interv Card Electrophysiol. https://doi.org/10.1007/s10840-021-00954-8

65. Kawaji T, Hojo S, Kushiyama A, Nakatsuma K, Kaneda K, Kato M, Yokomatsu T, Miki S (2019) Limitations of lesion quality estimated by ablation index: An in vitro study. J Cardiovasc Electrophysiol 30:926–933 . https://doi.org/10.1111/jce.13928

66. Huang ST, Dong JZ, Du X, Wu JH, Yu RH, Long DY, Ning M, Sang CH, Jiang CX, Bai R, Wen SN, Liu N, Li SN, Wang W, Guo XY, Zhao X, Chen X, Cui YK, Tang RB, Ma CS (2020) Relationship Between Ablation Lesion Size Estimated by Ablation Index and Different Ablation Settings—an Ex Vivo Porcine Heart Study. J Cardiovasc Transl Res 13:965–969 . https://doi.org/10.1007/s12265-020-10037-0

67. Avitall B, Mughal K, Hare J, Helms R, Krum D (1997) The effects of electrode-tissue contact on radiofrequency lesion generation. PACE - Pacing Clin Electrophysiol 20:2899–2910 . https://doi.org/10.1111/j.1540-8159.1997.tb05458.x

68. De Bortoli A, Sun LZ, Solheim E, Hoff PI, Schuster P, Ohm OJ, Chen J (2013) Ablation effect indicated by impedance fall is correlated with contact force level during ablation for atrial fibrillation. J Cardiovasc Electrophysiol 24:1210–1215 . https://doi.org/10.1111/jce.12215

69. LANGBERG JJ, LEE MA, CHIN MC, ROSENQVIST M (1990) Radiofrequency Catheter Ablation: The Effect of Electrode Size on Lesion Volume In Vivo. Pacing Clin Electrophysiol 13:1242–1248 . https://doi.org/10.1111/j.1540-8159.1990.tb02022.x

70. Nakagawa H, Wittkampf FHM, Yamanashi WS, Pitha J V., Imai S, Campbell B, Arruda M, Lazzara R, Jackman WM (1998) Inverse relationship between electrode size and lesion size during radiofrequency ablation with active electrode cooling. Circulation 98:458–465 . https://doi.org/10.1161/01.CIR.98.5.458

71. Rodrigo C. Chan, Susan B. Johnson, James B. Seward and DLP (2002) The effect of ablation electrode length and catheter tip to endocardial orientation on radiofrequency lesion size in the canine right atrium. PACE - Pacing Clin Electrophysiol 25:4–13 . https://doi.org/10.1046/j.1460-9592.2002.00004.x

72. Calzolari V, De Mattia L, Basso F, Crosato M, Scalon A, Squasi PAM, Del Favero S, Cernetti C (2020) Ablation catheter orientation: In vitro effects on

lesion size and in vivo analysis during PVI for atrial fibrillation. PACE - Pacing Clin Electrophysiol 43:1554–1563 . https://doi.org/10.1111/pace.14106

List of Publications and Award

International Journal

1. Masnok K., Watanabe N., (2021) Catheter contact area strongly correlates with lesion area in radiofrequency cardiac ablation: An ex vivo porcine heart study. J Interv Card Electrophysiol.
2. Masnok K., Watanabe N., (2021) Relationship of Catheter Contact Angle and Contact Force with Contact Area on the Surface of Heart Muscle Tissue in Cardiac Catheter Ablation. Cardiovasc Eng Tech 12, 407–417. https://doi.org/10.1007/s13239-021-00529-8

International Conference (Oral presentation)

1. Masnok K., Watanabe N., (2021) Role of Catheter Contact Force on Biophysical Properties of the Ablation Lesion Formation in Radiofrequency Catheter Cardiac Ablation. 2021 IEEE Region 10 Symposium (TENSYMP), Jeju, Republic of Korea, pp. 276-279.
2. Masnok K., Watanabe N., (2021) Effects of Increased Catheter Contact Force on the Ablation Impedance in the Radiofrequency Catheter Ablation of Cardiac Arrhythmias. 2021 IEEE 3rd Eurasia Conference on Biomedical Engineering, Healthcare and Sustainability (ECBIOS), Tainan, Taiwan, pp. 29-32, doi: 10.1109/ECBIOS51820.2021.9510226.
3. Masnok K., Watanabe N., (2021) Development of Experimental System which Enables to Set the Catheter Contact Angle and Contact Force for Study on Radiofrequency Catheter Ablation. The 15th South East Asian Technical University Consortium Symposium, Bandung, Indonesia.

Award

1. Masnok K., “Best Conference Paper Award” 2021 IEEE 3rd Eurasia Conference on Biomedical Engineering, Healthcare and Sustainability (ECBIOS), Tainan, Taiwan, 28th May 2021.

Curriculum Vitae

Kriengsak Masnok

2018 – Present	**Ph.D. Student in Functional Control Systems**, Shibaura Institute of Technology, Japan.
	Thesis: Investigation of Catheter's Contact Force and Angle Effects on Contact Area and Lesion Size in Radiofrequency Catheter Cardiac Ablation.
	Supervisor: Assoc. Prof. Dr. Nobuo Watanabe
2017 – 2018	**M.Sc. in System Engineering and Sciences**, Shibaura Institute of Technology, Japan.
2015 – 2017	**M.Eng. in Industrial Engineering**, Suranaree University of Technology, Thailand.
2010 – 2014	**B.Eng. in Industrial Engineering**, Suranaree University of Technology, Thailand.